Fall Field Frolic 2012 (August 22-25)
'Mother Lode to Walker Lane'

Itinerary:

DAY 1: Wednesday, August 22. Depart Lot G3 @ CSUN at 8 AM.

- Stop for lunch ~ 12:30 in Merced, CA
- Stop 1-1: Calaveras Complex outcrop and swimming on the Stanislaus River (~4 PM)
- Camp at Glory Hole Ironhorse Camps 64, 67-69 at New Melones Reservoir.

DAY 2: Thursday, August 23. Leave camp promptly at 7:30 AM, and take CA49 through the foothills to Grass Valley.

- Stop 2-1: 10:30 tour of the Empire Mine in Grass Valley. Lunch at the mine.
- Stop 2-2: ~ 2 PM; Malakoff Diggins State Park NE of Grass Valley.
- Camp at Packsaddle Camps 8-12 in Sierra Buttes near Sardine Lake.

DAY 3: Friday, August 24. Drive from the Sierra Buttes to Grover Hot Springs via Graeagle and Lake Tahoe.

- Stop 3-1: Short (~3 mile) hike to visit Paleozoic volcanic-arc sequences and glacial geology in the Lakes Basin. Drive to Graeagle for lunch by the river.
- Stop 3-2: Fallen Leaf Lake near south Lake Tahoe
- Camp at Grover Hot Springs Sites 7-10

DAY 4: Saturday August 25. Drive home over Monitor Pass and through the Owens Valley. We will make one stop at Convict Lake to observe the truncated moraines. Arrive CSUN late Saturday evening.

Overview map of Fall Field Frolic 2012. Blue markers inticate the starting point (CSUN) and campsite locations. Details of stops are shown in the text.

California Geography Overview

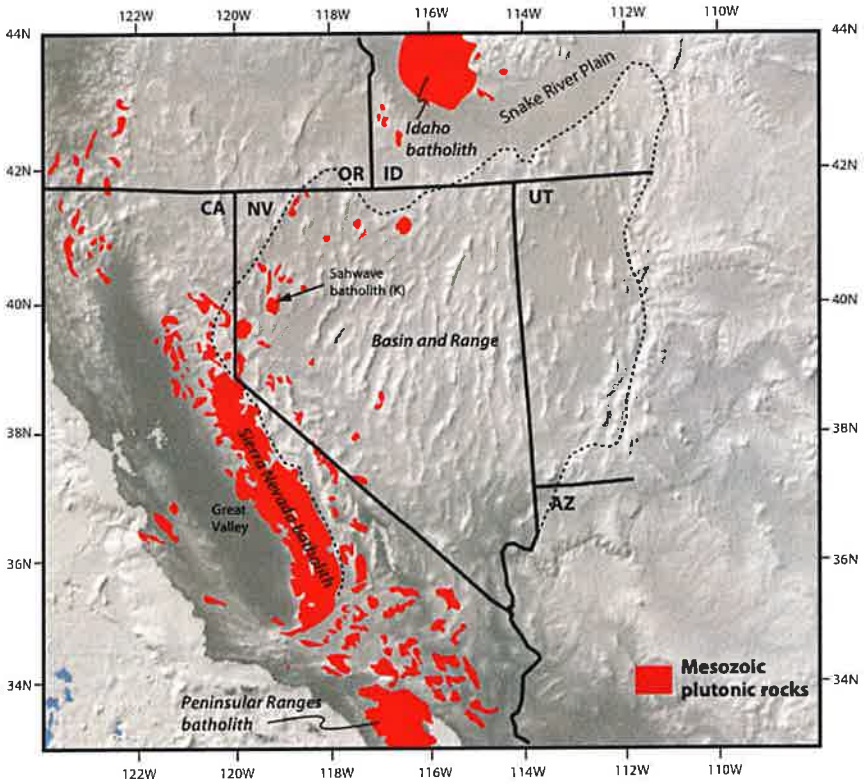

Batholithic rocks of the Sierra Nevada. Note the fragmentation and dispersion of the batholith to the North.

Day 1: Drive to the central Sierra Nevada foothills, stopping in Merced for lunch. From Merced, we will make our way north and east to the Melones Reservoir.

Stop 1-1: View the Calaveras Fm near the Camp 9 swimming hole on the Stanislaus River. The Stanislaus is one of the major east – west drainages that dissects the westward-tilted Sierran block. A map of major west-flowing Sierran rivers is given below. The Yuba and Feather River drainages that we'll see tomorrow are to the north of the American River.

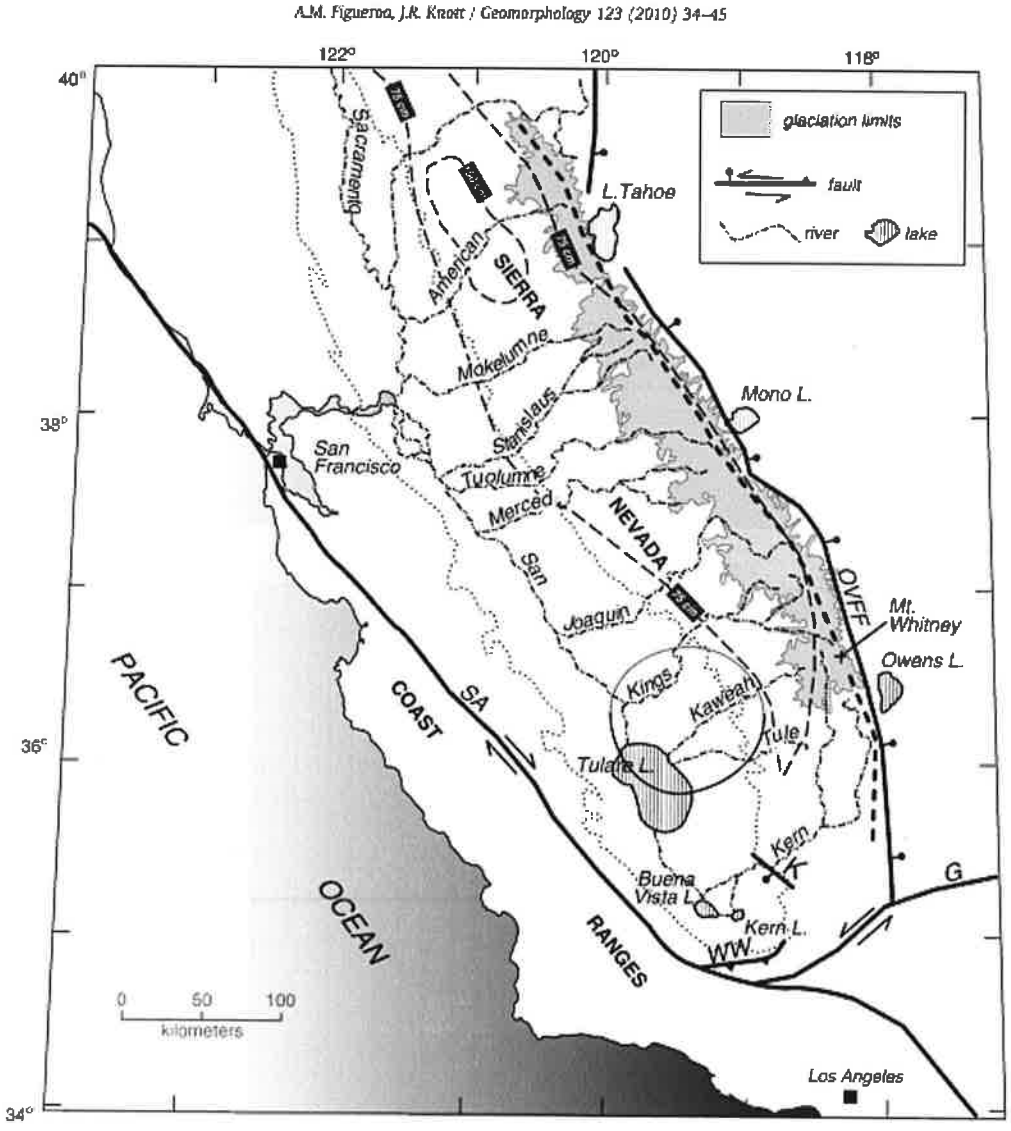

The Calaveras Formation is one of the major units making up the western metamorphic foothills belt of the Sierra Nevada. More about the foothills belt is given on the next page.

Foothills Metamorphic Belt

(text modified from a field trip guide by C. Merguerian, Hofstra University)

The foothills metamorphic belt of the western Sierra Nevada is roughly 350 km long, 60 km wide and extends from lat. 40°15'N south-southeasterly to lat. 37°N. It is overlain by Cretaceous to Cenozoic rocks of the Great Valley sequence to the west and is intruded by the Sierra Nevada batholith to the east (see generalized geologic map of California below). It comprises three ductile-fault bounded tectonostratigraphic units known as the Jurassic belt, the Calaveras Complex, and the Shoo Fly Complex. These contiguous belts show an eastward increase in age, metamorphic grade, and structural complexity with abrupt lithologic, structural, and metamorphic truncations occurring at the Melones, Sonora, and Calaveras-Shoo Fly faults.

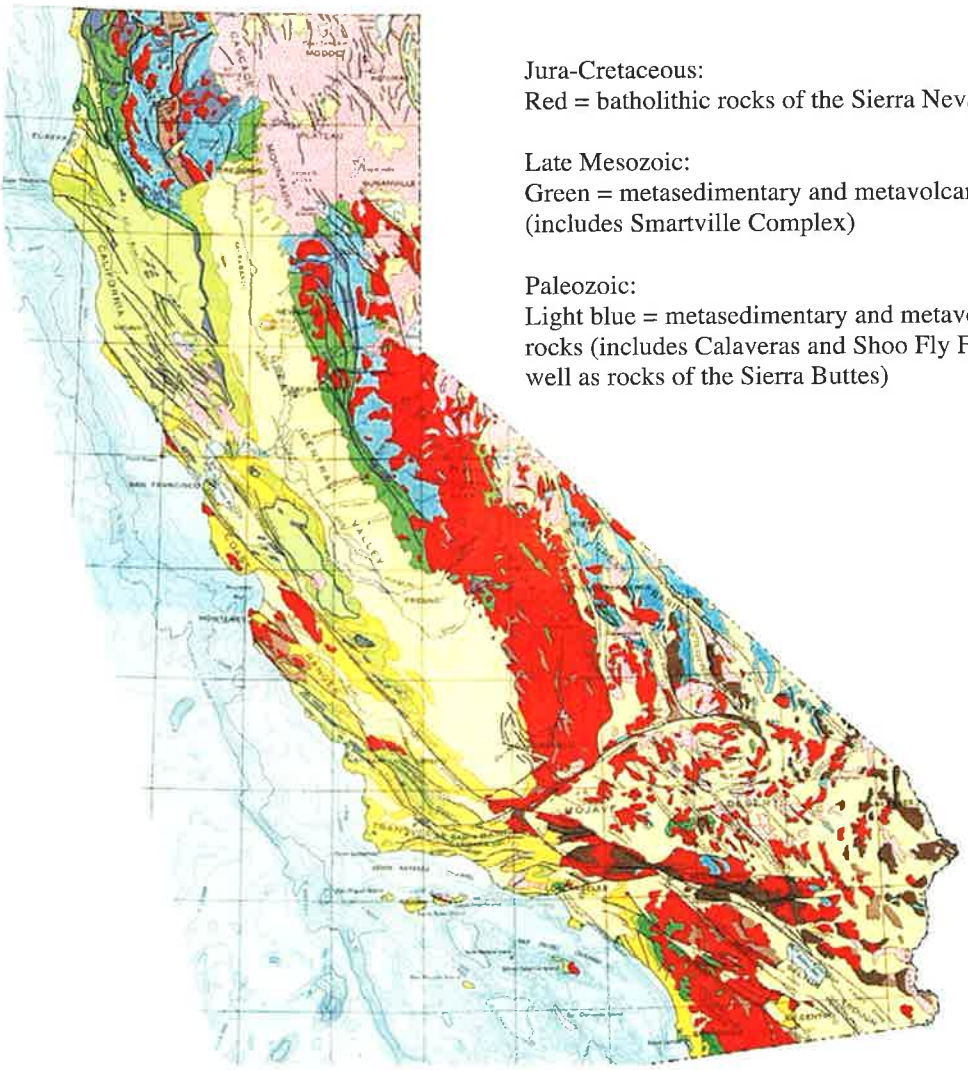

Jura-Cretaceous:
Red = batholithic rocks of the Sierra Nevada

Late Mesozoic:
Green = metasedimentary and metavolcanic rocks (includes Smartville Complex)

Paleozoic:
Light blue = metasedimentary and metavolcanic rocks (includes Calaveras and Shoo Fly Fms, as well as rocks of the Sierra Buttes)

The lower Paleozoic **Shoo Fly Complex** underlies a terrane 330 km in length and 6-20 km wide which terminates southward near latitude 37°30'N in Mariposa County, where batholithic rocks cut across trend (near Bass Lake, east of Fresno). The Shoo Fly Complex shows a marked southward increase in structural complexity and metamorphic grade. North of lat. 39°N it consists of weakly metamorphosed quartzose sandstone, graywacke, slate, chert and limestone. South of lat. 38°05'N, it is a multiply deformed and sheared assemblage of quartzite, quartzofeldspathic gneiss, granite-, syenite-,and gabbroic augen gneiss, garnet schist, calc-silicate rock, marble, and rare amphibolite.

The Shoo Fly is in ductile fault contact with the Permo-Triassic **Calaveras Complex.** The Calaveras, which forms the lower plate of the east-dipping thrust, is a chaotic assemblage of massive argillite and siltstone, marble, massive and rhythmically bedded-chert, talc-schist, basalt, and rare sandstone layers. We will drive through marbles of the Calaveras on our way to the Stanislaus river, where we look at an outcrop of massive cherty argillaceous rocks.
The westernmost **Jurassic Belt** comprises Jurassic island arc volcanic and volcaniclastic strata and deep-water flysch-type sediment. Cropping out east of the Central Valley where flat-lying strata predominate, tilted and cleaved metasedimentary and metavolcanic rocks of Jurassic age form an impressive former volcanic arc terrane now exposed in dissected low rolling hills that reflect the trend of the lithologic units and bounding faults. These rocks were isoclinally folded and cleaved under chlorite to greenschist grade metamorphic conditions in contrast to the blueschist metamorphism found in the Coast Range.

Cut by major faults in the vicinity of Jamestown, where slivers of serpentinite exhibit shearing and multiple offsets, the Jurassic Belt is in fault contact with deformed Permo-Triassic marble and chaotic argillite of the Calaveras Formation along the Melones or Sonora faults (see map and cross section on next page). The Calaveras, in turn, is in ductile fault contact with the lower Paleozoic Shoo Fly Complex along the Calaveras-Shoo Fly thrust. Thus, in cross sectional view the foothills metamorphic belt consists of a sequence of fault steeply dipping fault bounded terranes of increasing age, metamorphic grade, and structural complexity from west to east.

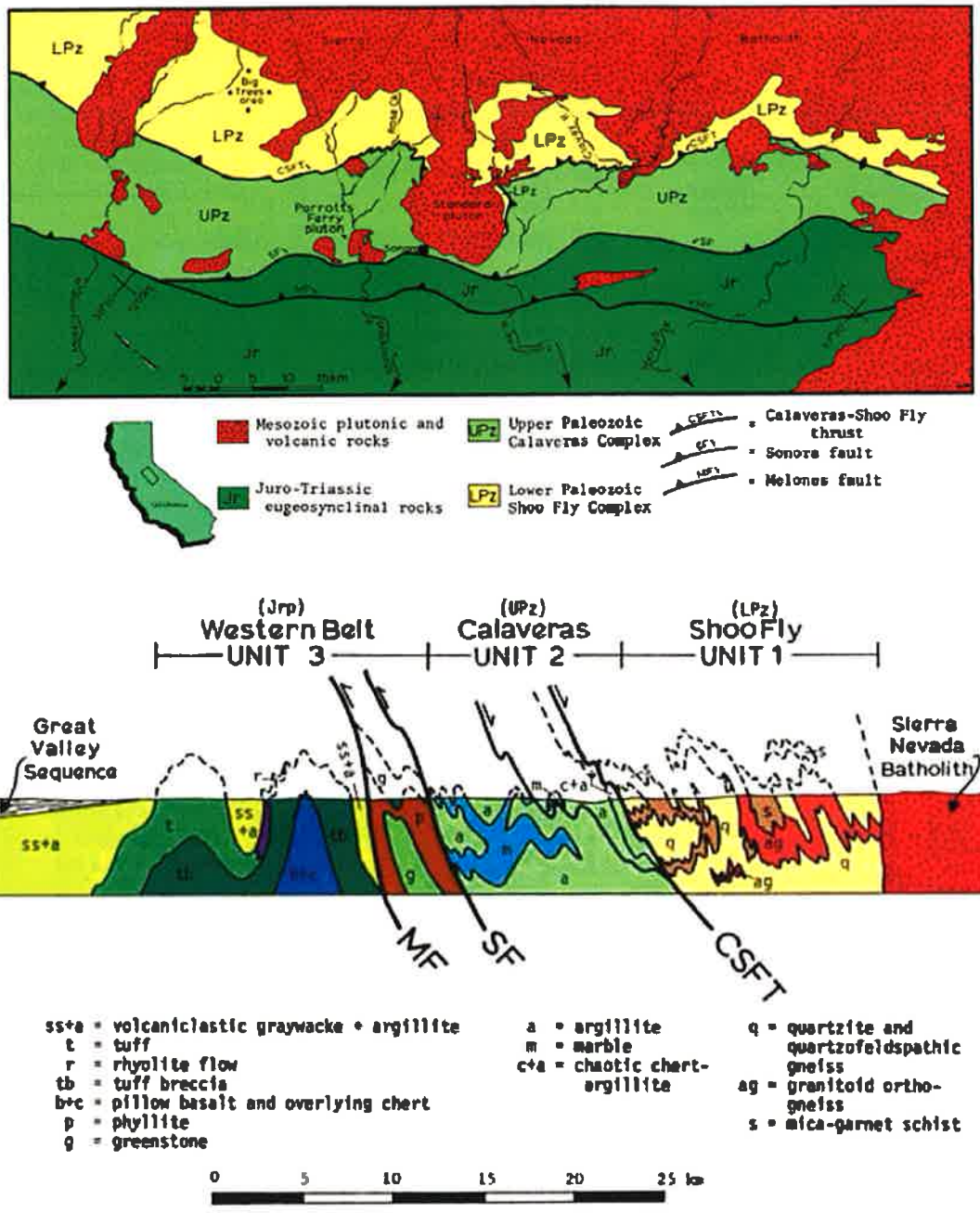

From Merguerian, 1985

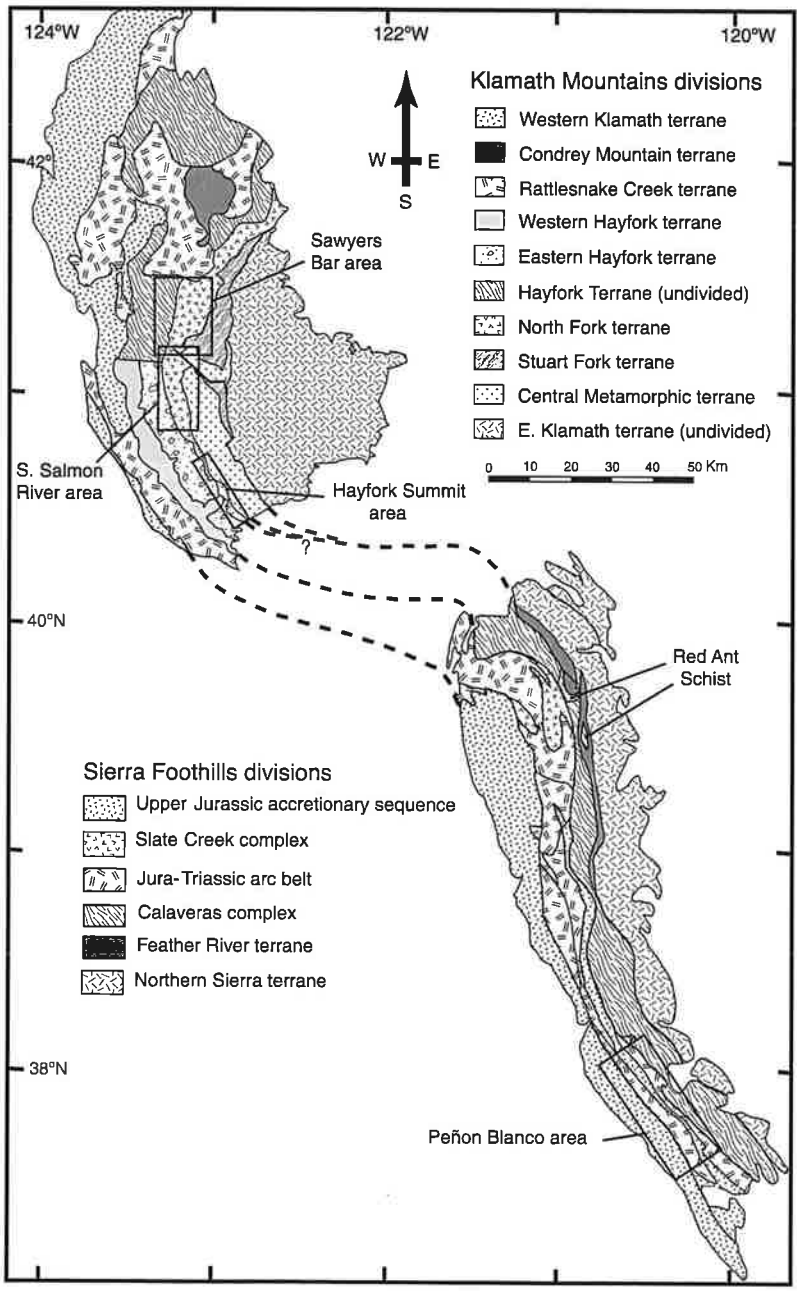

Fig. 1 Generalized geological map of the Klamath Mountains and the western Sierran Foothills, after Irwin (1981, 2003), Sharp (1988), Edelman and Sharp (1989), Ernst (1998) and Snow and Scherer (2006). The Sawyers Bar, South Salmon River, Hayfork Summit, and Peñon Blanco areas are indicated.

Petrotectonics of the North Fork terrane

Main North Fork rock types (Irwin, 1972, 1994) include serpentinized ultramafic, metagabbroic, metabasaltic, metasedimentary and volcaniclastic metasedimentary rocks; abundances vary along strike of the belt. Contacts between the units follow the arcuate, NS regional trend. Geological mapping in the North Fork terrane south of the Salmon River by Ando *et al.* (1983) identified a tectonically disrupted mafic–ultramafic basement complex, overlain by a superjacent series consisting of chert, argillite, volcanic rocks and massive limestone. On the basis of field and geochemical data, Ando *et al.* viewed this South Salmon River complex as a disrupted MORB-type ophiolite, possibly a seamount.

North of the Salmon River, mapping and geochemical analysis of the Sawyers Bar area (Fig. 2; Ernst *et al.*, 1991; Ernst, 1998) led to the recognition of three interstratified superjacent units in the central North Fork terrane: St. Clair Creek distal turbidites and interlayered cherts; North Fork *sensu stricto* ocean-island amygdaloidal basalts, pillow basalts and flow breccias (OIBs); and massive to pillowed Salmon River island-arc tholeiitic basalts and intrusives (IATs). Serpentinized peridotite is common, especially along terrane-bounding faults. Hacker *et al.* (1993) contrasted the more coherent St. Claire Creek argillites with the relatively disaggregated chert + argillite mélanges of the outboard Eastern Hayfork terrane. Both sedimentary units are interbedded with mafic igneous rocks petrologically similar to North Fork *sensu stricto* and Salmon River basalts. Intimate stratigraphic interlayering of mafic flows and sediments and pillow tops in the North Fork terrane suggest development in an oceanic arc, as supported by OIB and IAT bulk-rock geochemistry (Ernst *et al.*, 1991). Distal argillaceous turbidites chiefly underlie the basaltic pile at Sawyers Bar. Based on the petrography of St. Clair Creek siltstones, clasts apparently were derived from eastern Klamath terranes. Ernst (1999a) concluded that the mafic volcanogenic section formed near the continental margin directly outboard from the Klamath accretionary arc, rather than in the open ocean as proposed by Ando *et al.* (1983) for the North Fork terrane to the south.

In the southernmost, Klamath Mountains (Wright, 1982) showed that the North Fork assemblage is petrotectonically similar to the Eastern Hayfork, consisting of a chert-rich metasedimentary sequence resting on a mafic–ultramafic basement. Wright considered the metavolcanic unit as MORB that had been transported continentward, became disrupted and included in serpentinite matrix mélange, and was then overlain by Upper Triassic–Middle Jurassic sedimentary strata. Locally, OIB metavolcanic

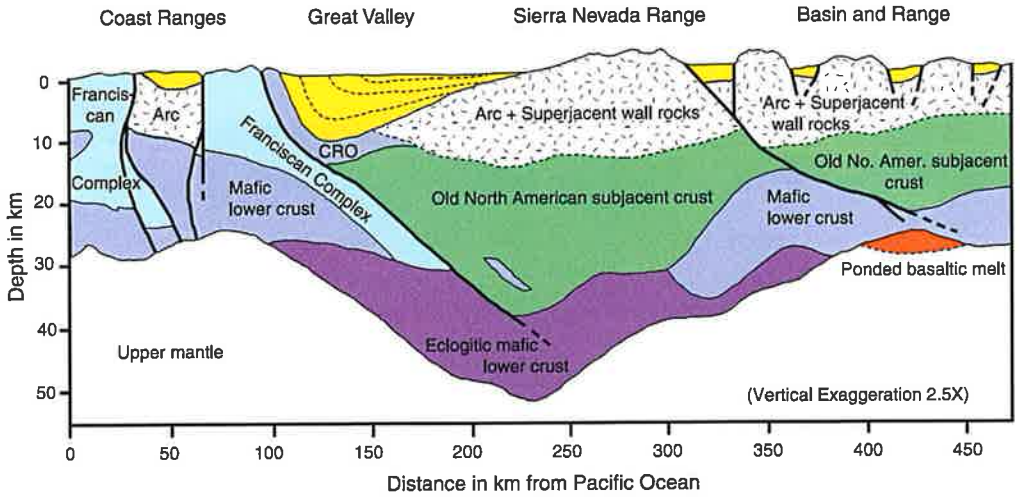

Fig. 7 Diagrammatic EW cross-section through central California based on geophysical data (Fliedner *et al.*, 2000), petrochemistry (Ducea and Saleeby, 1998a,b) and general geology (Ernst *et al.*, 2003). Mid-Paleozoic to mid-Mesozoic accreted ophiolitic chert–argillite terranes (superjacent wall rocks) were transported along and sutured against the Californian margin during a *c.* 230 Myr. span by dominantly transtensional + transpressional slip approximately normal to the plane of section. In contrast, chiefly Cretaceous growth of the Klamath–Sierran calcalkaline volcanic–plutonic arc and derivative coeval forearc basin + trench deposits resulted from *c.* 70 Myr. of mainly head-on subduction. Terranes are duplicated in the Coast Ranges reflecting Neogene dextral slip along the San Andreas system.

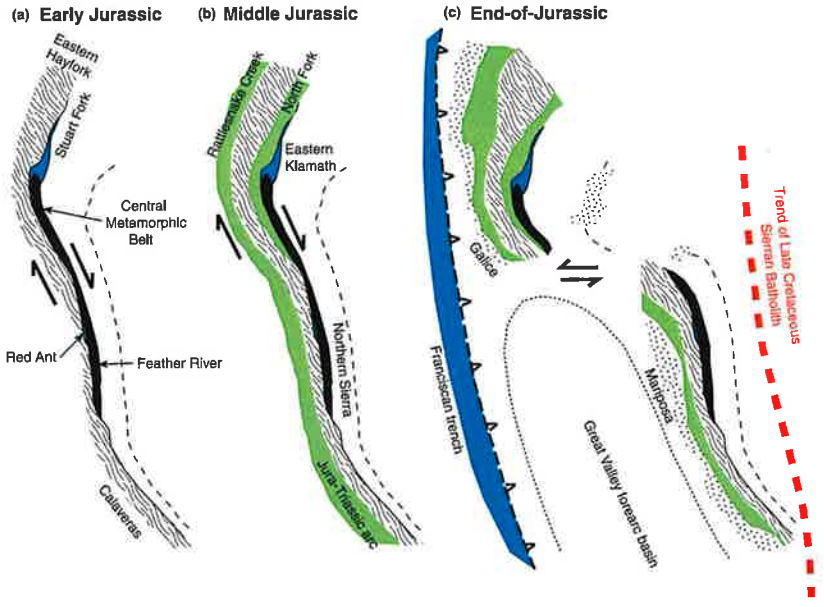

Fig. 8 Speculative plate-tectonic scenario for the Jurassic evolution of northern and central California, assuming dextral strike slip along the continental margin (but see Avé Lallemant and Oldow, 1988; and Anderson, 2007 for a sinestral interpretation) and end-of-Jurassic westward displacement of the Klamath salient, similar to the modern San Andreas–Garlock fault slip system. Relationships are slightly modified from Ernst *et al.* (2008): (a) transcurrent suturing of the Eastern Hayfork–Calaveras amalgam at *c.* 205–195 Ma; (b) rifting and spreading of the medial Klamath terrane assembly with oceanic crust produced and/or tectonically inserted both outboard (Rattlesnake Creek) and inboard (North Fork) of the Eastern Hayfork terrane at *c.* 190–170 Ma, followed by transpression, hot hanging-wall metamorphism of high-grade Franciscan blueschists ± eclogites at *c.* 155 Ma, incipient landward arc formation and deposition of the Galice–Mariposa formations (not illustrated) during westward extrusion of the Klamath salient; (c) westward step out of a new transpressive-to-convergent plate junction at *c.* 145–150 Ma. Subduction-zone-generated massive volcanism–plutonism during mid- and Late Cretaceous time produced an Andean-type calcalkaline arc directly east of the Sierran Foothills; the red dashed line shows the trend of the batholith, after the map compilation by Irwin (2003). The northern extension of the arc was sited well to the east of the Klamath salient, but has been eroded and/or covered by Cenozoic volcanic rocks of the Cascade and Modoc Plateau provinces.

Day 2: Break camp and get on the road by **8 AM**, sharp!! Enjoy a beautiful and twisty drive up the famous motherlode highway (CA49). Our journey will end at our first stop of the day, the Empire Mine (reminder: $9 / person fee for taking the mine tour).

Stop 2-1: Tour of the Empire Mine, one of the largest hard-rock gold mines in motherlode country.

Brief History: The Empire Mine was the richest hard-rock mine in the State of California producing 5.8 million ounces of gold in its operating history of 106 years (1850-1956). George Roberts, the original discoverer of the gold soon sold his interest and by 1869 William Bourn Sr. owned controlling interest. The Bourn family maintained control of the mine until 1929 when it was sold to Newmont Mining. It ceased operation in 1956. In 1975 the State purchased the surface property as the Empire Mine State Historic Park. The Park continues to draw thousands of worldwide visitors each year and is noted for its historical tours of the Bourn Cottage, the mineyard and "living history" events.

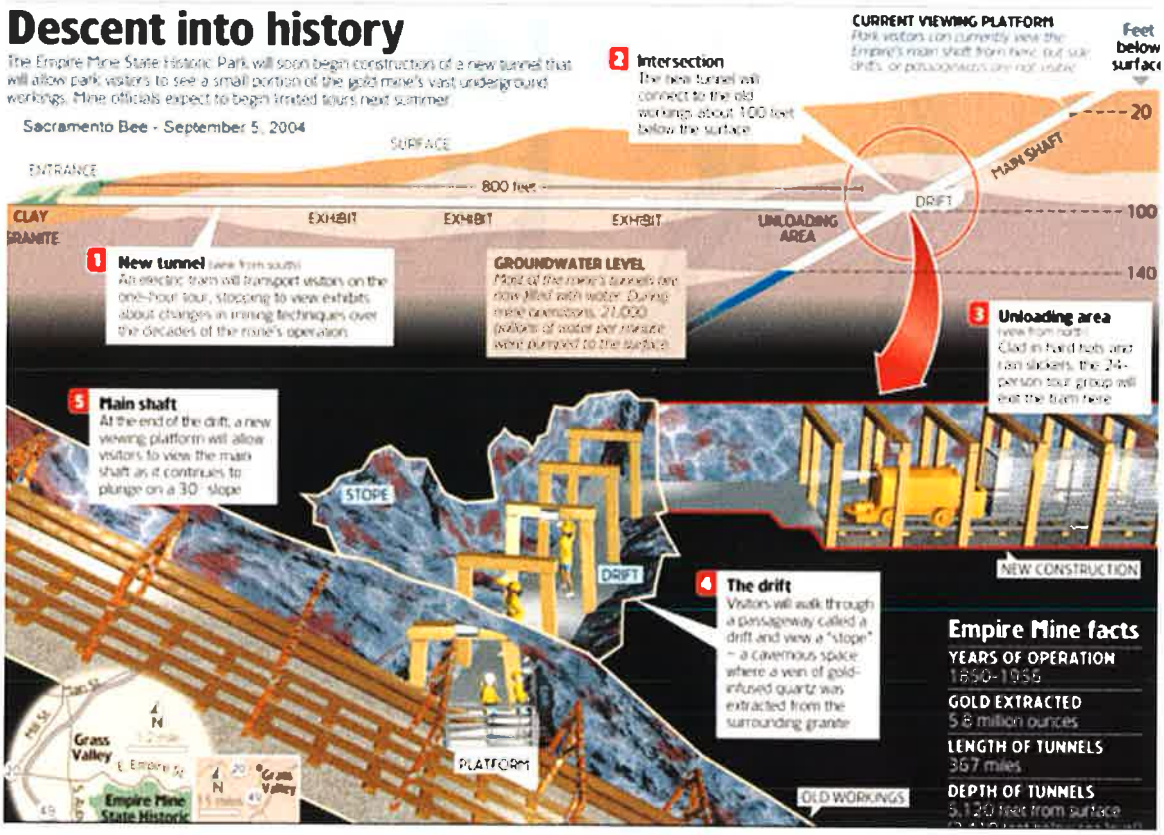

Stop 2-2: After the tour, we will eat lunch in the shady picnic tables at the mine before driving to the Malakoff Diggins. Malakoff is an abandoned hydraulic mining pit (now a state park), where placer gold was blasted out of Eocene – earliest Oligocene (?) fluvial gravels. Malakoff is one of several hydraulic pits, shown on the map on the next page. These gravels are important players in understanding the Cenozoic tectonic and geomorphic evolution of the Sierra Nevada. Some text explaining that is inserted below (from Cecil et al., 2010).

The range bears an asymmetrical profile with a steeply sloping eastern margin and a more gently dipping western margin, which has long been interpreted to be the result of westward block tilting [e.g., Lindgren, 1911; Christensen, 1966; Huber, 1981; Unruh, 1991]. Westward tilting, initiated by the development of the east side-down normal faults along the Sierran front, is thought to have generated uplift at the range crest since the time of faulting (circa 5 Ma [Wakabayashi and Sawyer, 2001]). The degree to which the Sierra has been tilted and the amount of surface uplift interpreted to have occurred in the late Cenozoic, however, remains controversial.

[3] Many datasets have been brought to bear on this issue of recent range-wide uplift. Geomorphic reconstructions of paleochannels preserved in the western Sierra have been used to argue for an increase in slope following Eocene through Miocene deposition of sediments in the channels [Lindgren, 1911; Hudson, 1955, 1960; Huber, 1981, 1990; Jones et al., 2004]. A marked increase in downcutting rates of southern Sierra rivers from ~1.3 to 2.7 mm/yr at circa 3 Ma has also been suggested as evidence of an additional phase of Late Cenozoic surface uplift and incision [Wakabayashi and Sawyer, 2001] into significant preexisting topography [Stock et al., 2005, 2004]. Late Cenozoic surface and/or rock uplift is not reflected in low-temperature thermochrono- metric data, however, which indicate protracted range-wide long-term exhumation rates in the mid-Cenozoic [House et al., 2001; Clark et al., 2005; Cecil et al., 2006]. In fact, the distribution of variable (U-Th)/He ages across modern can- yons in the south central Sierra has been used to argue for the presence of high-relief paleocanyons in the Paleogene, implying a decrease in relief and crestal elevations since ~60 Ma [House et al., 1998; Braun, 2002].

[4] Stable isotope geochemistry has been used to both constrain the timing of a rain shadow effect in the Great Basin east of the Sierra Nevada [Poage and Chamberlain, 2002], and to estimate paleoaltitudes of the Sierra Nevada–Great Basin region [Horton et al., 2004; Mulch et al., 2006, 2008; Crowley et al., 2008; Cassel et al., 2009a; Hren et al., 2010]. Those data indicate the presence of a Miocene rain shadow and Eocene through Pleistocene western gradients similar to present day, which is difficult to reconcile with earlier geomorphic studies. Paleoaltimetric studies strengthen the case for a high interior upland (termed the Nevadaplano [DeCelles, 2004]) existing to the east of the Sierra Nevada [Horton et al., 2004; Cassel et al., 2009a]. It should be emphasized, however, that these seemingly contradictory data sets are complicated by the fact that the northern (north of 37.5°N) and southern parts of the Sierra Nevada are markedly different in many respects and may not share a common topographic evolution.

[5] The paleotopography of the northern Sierra Nevada and the paleotopographic and geodynamic relationship between the ancestral Sierra and the Nevadaplano to the east remain unclear, partly due to deformation east of the Sierra Nevada associated with the westward encroachment of Basin and Range faulting, and the relative paucity of Cenozoic geology preserved within the Sierra. We present new detrital zircon U-Pb and (U-Th)/He ages from Eocene river sedi- ments, which we use to assess the relative contributions of sediment sources from within the Sierra Nevada and basement terranes to the east. Our aims are twofold: (1) to constrain the upstream drainage areas of paleorivers and (2) to estimate the position of the Eocene drainage divide. Such analyses allow us to estimate depositional gradients and to create a model of large-scale range paleotopography. These issues have implications for the rock and surface uplift history of the Sierra Nevada, which is key to determining the geodynamic processes responsible for the creation and/or maintenance of high topography over geologic timescales.

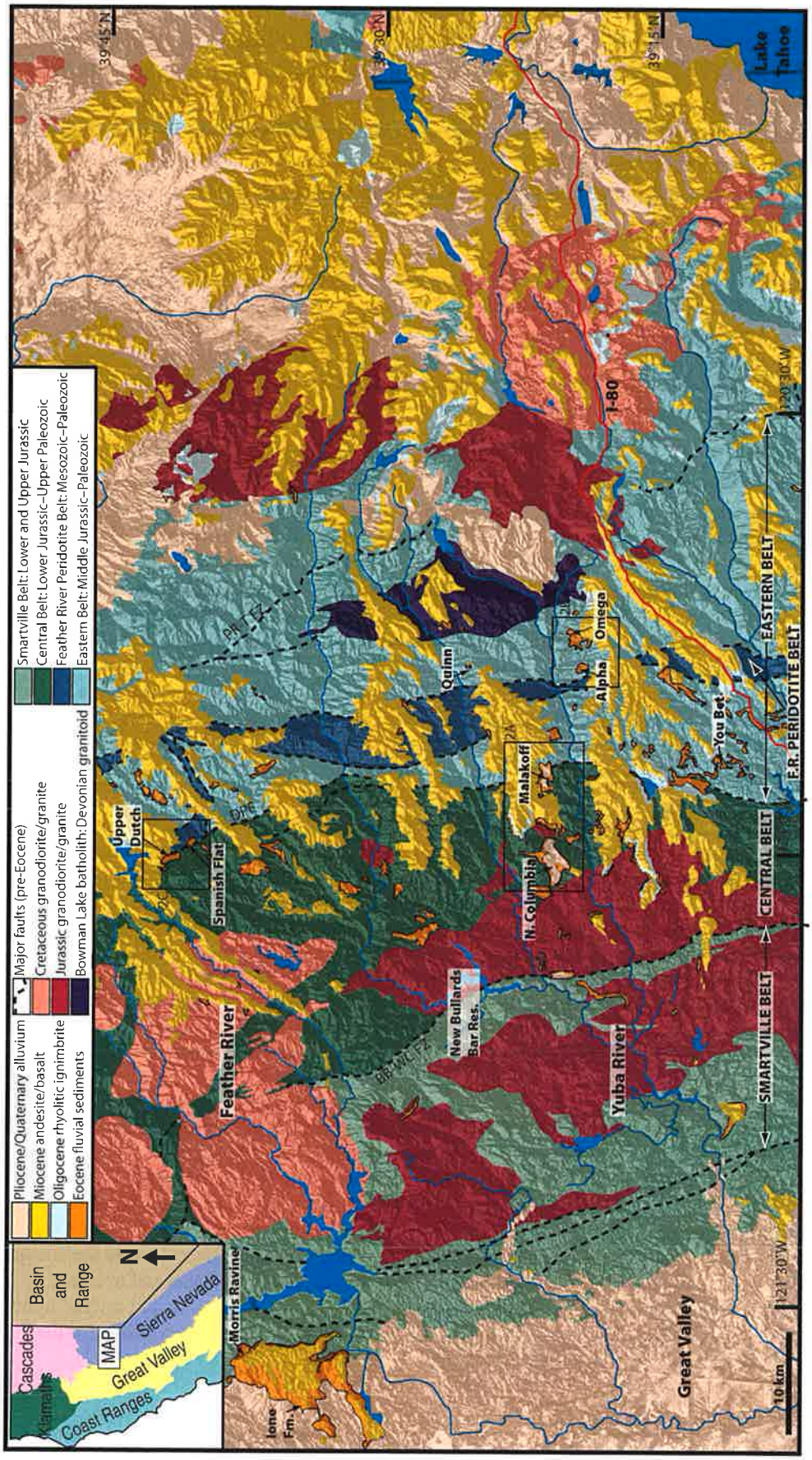

Figure 1. Distribution of geologic units in the northern Sierra Nevada of California (Interstate Highway 80 is shown in red for reference); inset shows map location and major tectonic regions of northern California and Nevada. The Big Bend–Wolf Creek fault zone (BB-WC FZ), Pinoli Ridge–Talbot fault zone (PR-T FZ), Dogwood Peak fault (DPF), and other faults, shown with black dashed lines, divide north-south–trending bedrock belts. Distribution of Eocene fluvial sediments is shown in orange, with important field locations for this study noted. Black boxes show locations of Figures 2A, 2B, and 2C. Digital elevation model is from U.S. Geological Survey Seamless Data Warehouse; geology is based on Yeend (1974), Saucedo and Wagner (1992), and Girty et al. (1996).

Generalized stratigraphy and interpretation of detrital zircon data and sedimentologic analysis of the gravels are given in the following figures.

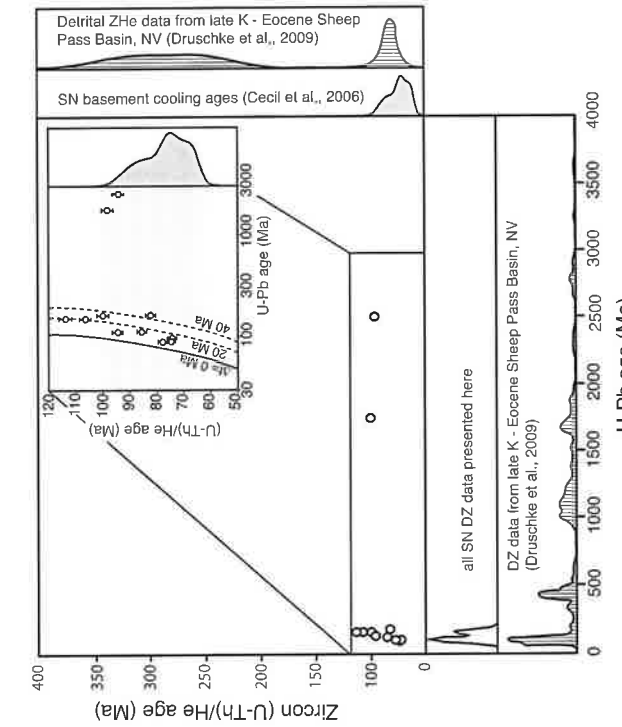

Detrital U-Pb and (U-Th)/He double dates of zircon grains from the Blue Lead sand sample (3a; Figure 2). (U-Th)/He ages are compared to (U-Th)/He zircon ages from Sierran bedrock samples (curve at right [from Cecil et al., 2006]) and to detrital (U-Th)/He cooling ages of zircons from the late Cretaceous-Eocene Sheep Pass Basin, east central Nevada [from Druschke et al., 2009]. U-Pb ages are compared to both the total distribution of detrital zircon ages measured here (Precambrian grains are of such low relative abundance that they do not plot visibly) and detrital zircon ages from the Sheep Pass Basin [Druschke et al., 2009]. For clarity, our double-dated grains are shown again at different scale in the inset. U-Pb ages in the inset are plotted on a logarithmic scale. At such a scale, error bars are not visible. Zircon (U-Th)/He ages lie below, and are parallel to, the 1:1 He/Pb line (difference between crystallization and cooling age is zero; Dt = 0 Ma), as is expected for plutonic samples. Most grains fall within Dt contours drawn at 20 Ma and 40 Ma, indicating rapid cooling in the late Cretaceous, which is consistent with interpretations of bedrock cooling ages. Two multicycle grains (defined as those grains having Dt > 300 Ma [Campbell et al., 2005]) have similar cooling ages, suggesting a common exhu- mation history. This is in contrast to similar ages detritus in Nevada, which has both Cretaceous and Permian cooling ages. From Cecil et al., 2012: Tectonics

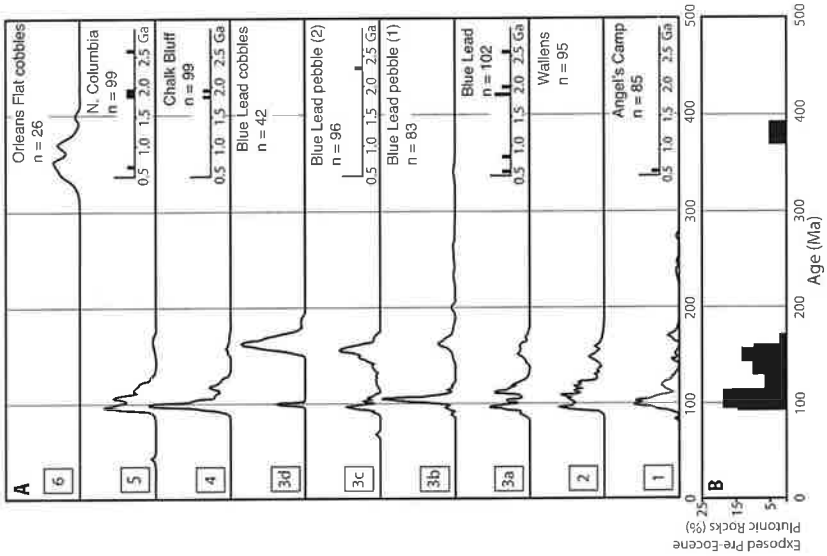

Detrital zircon age spectra for Eocene paleoriver deposits. (a) Data are plotted at two scales to emphasize the Mesozoic populations. Relative probability curves for Phanerozoic ages are plotted from 0 to 500 and inset are histograms of older grains plotted from 500 to 3000 Ma. (b) Relative age distribution of exposed pre-Eocene plutonic rocks in the northern Sierra Nevada (box in Figure 3). From Cecil et al., 2012: Tectonics

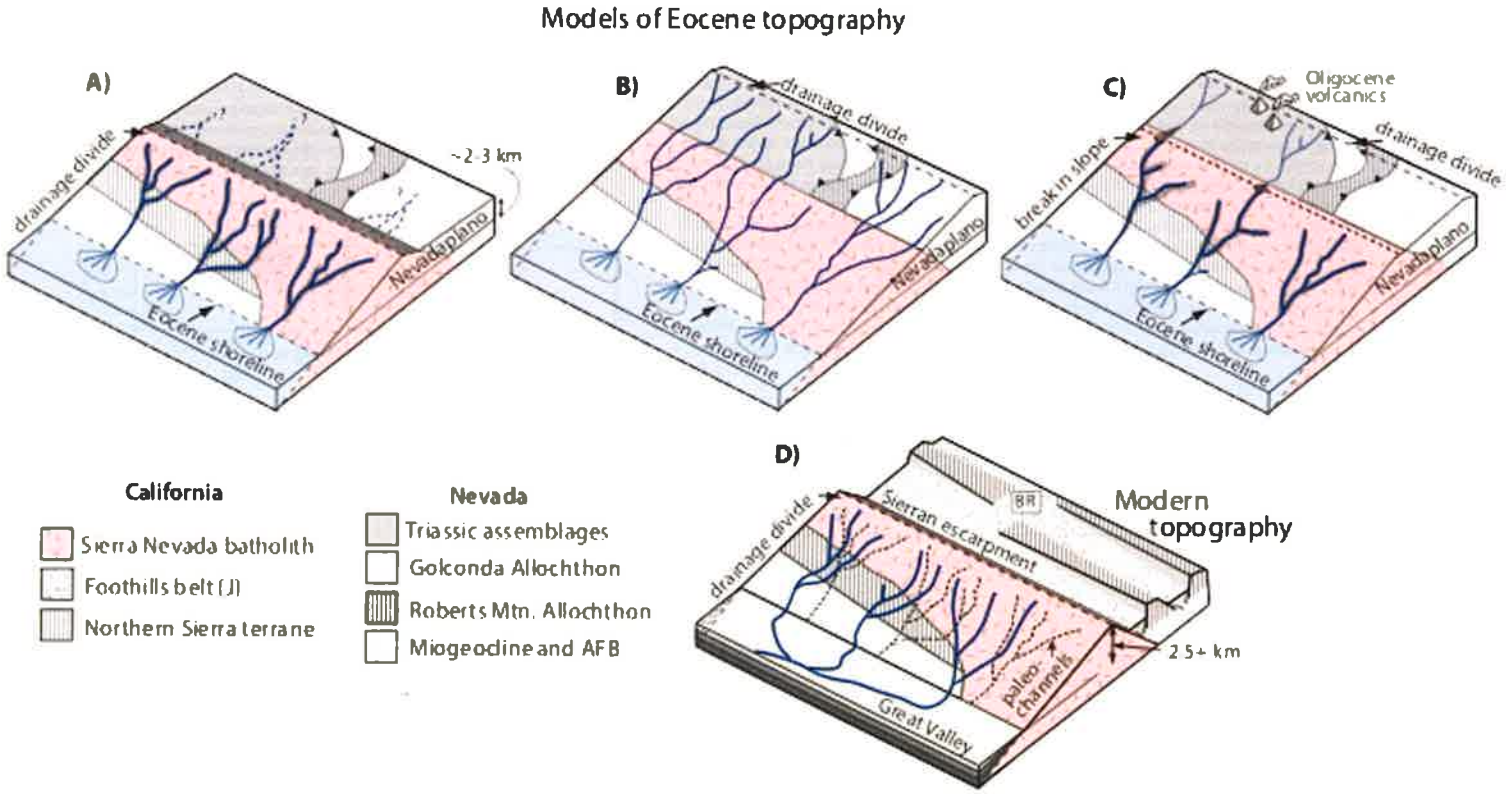

Schematic block models representing (a–c) Eocene and (d) modern topographic configura- tions of the Sierra Nevada and adjacent Nevada highlands (Eocene/Basin and Range (modern). Figure 8a shows paleotopography of the Sierra Nevada best supported by the detrital zircon data presented herein. A drainage divide, in roughly the same position as that of the modern one, separates the Sierra from the interior Nevadaplano. Paleorivers are relatively steep, with small catchments, sourced entirely within the Sierra Nevada block. Crestal elevations are assumed to be at least 1.5 km, based on paleoelevation esti- mates for the Nevadaplano. The western flank of the Sierra slopes westward at a gradient similar to the modern one. Figure 8b shows traditional model of Sierra Nevada paleotopography based on a regionally developed erosion surface and the meandering and alluviated nature of Eocene rivers. This model implies a shallow gradient for the western Sierran flank, with relatively low-slope rivers draining a large area, and is a poor fit to the detrital zircon data presented here. In Figure 8c paleorivers drain westward across the Nevadaplano in nonerosive channels but must incise and exclusively incorporate Sierran detritus to the west to be consistent with our provenance data. This model requires a change in slope or some other mechanism for changing erosive power of the paleorivers at or near the modern divide but has the benefit of not requiring a large (>150 km) eastward shift in drainage divide position before deposition of Oligo- cene ash flows in Sierran paleorivers. In Figure 8d the period from ~5 Ma to the present is marked by the extensional collapse of the nearby Nevada highlands and the development of the Sierran frontal escarp- ment, perhaps accompanied by moderate uplift of the range crest. Paleochannels (gray dashed) are aban- doned, and modern drainages (dark blue) are incised. BR, Basin and Range. From Cecil et al., 2010, Tectonics.

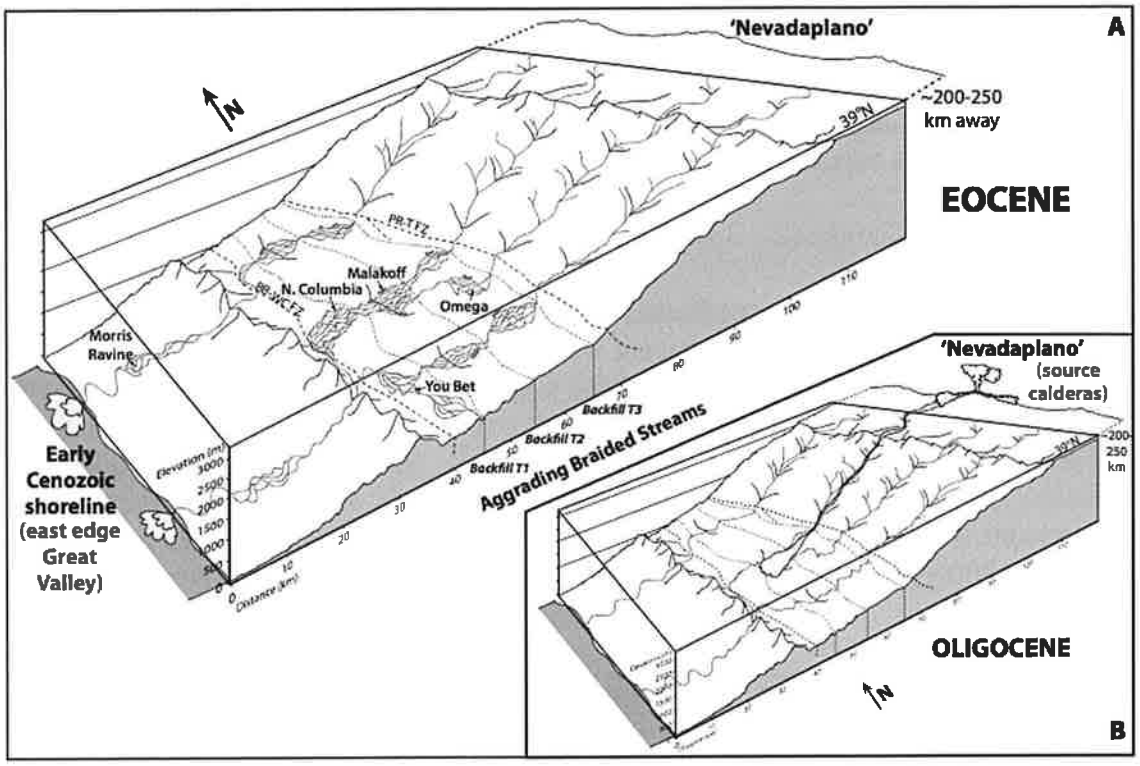

Figure 13. Schematic reconstruction of area that is now the northern Sierra Nevada. (A) Eocene: rivers incising in high-elevation areas in steep, high-gradient paleovalleys, feeding sediment into braided streams aggrading in broad, lower-gradient paleovalleys. Dashed lines indicate pre-Cenozoic fault zones that delineate the depositional area (BB-WC—Big Bend–Wolf Creek; PR-T—Pinoli Ridge–Talbot); arrows indicate locations of selected study areas (Fig. 1). Thin fine-dashed lines indicate proposed backfilling sequence progressing from west to east; the locus of deposition and channel patterns likely shifted between these intervals. (B) Oligocene: ignimbrites originating from calderas ~200–250 km to the east (now central Nevada) deposited in the northern Sierra Nevada. Elevation estimates and Oligocene reconstruction are based on previous studies (see text for citations).

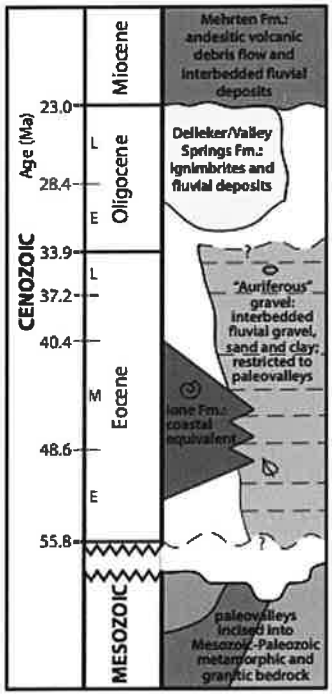

Figures from Cassel et al., 2011: GSAB

After Malakoff, we will continue up Hwy 49 to the Lakes Basin, where we will camp for the night.

Day 3: Pack up in the morning and drive a very short distance to a Lakes Basin trailhead. Be prepared for an easy, beautiful, 2.5 mile hike. On this hike, we will discuss the glacial history of the Sierra Nevada and the geology of the Sierra Buttes.

Stop 3-1: Lake Basin hike (2 – 3 hours of hiking, smiling, and chatting).

The glacial history of the Sierra Buttes has not been well-studied, although many other parts of the Sierra Nevada have a well-documented glacial history. This history has been determined by dating the sequence of nested moraines within glaciated valleys. Moraines are ridges of rock debris, called till, that are deposited on the margins of active glaciers (see photo below). Younger, more recent glacial moraines are inset into older moraine ridges. Over time, moraines degrade and develop soil. Moraines from the last glacial maximum, that occurred between 25,000-15,000 years ago, are well preserved in the high Sierra at places such as Sardine Lake.

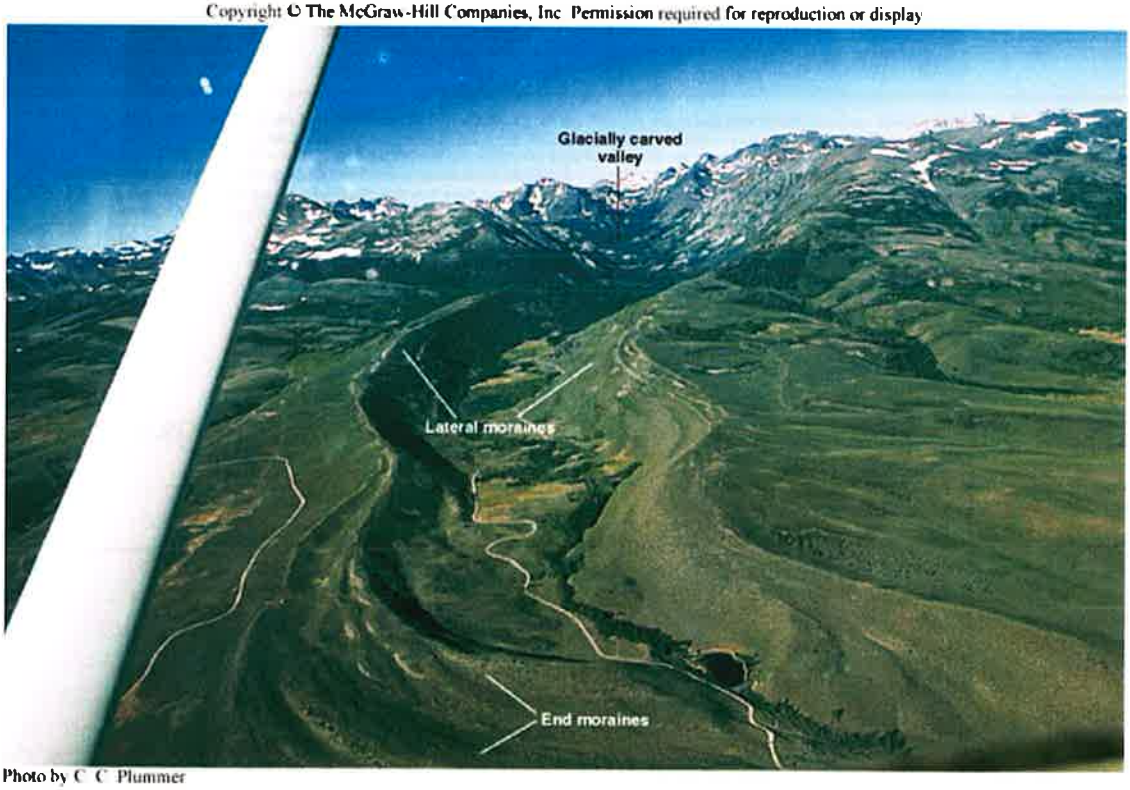

Photo by C C Plummer

Examples of well-studies glacial moraines within the Owens Valley just north of Bishop, CA. Inset moraines are younger and often better preserved (ie. sharp crests, less weathered boulders) than the outer, older moraines, and suggest more recent glacial advances.

Dating of moraines and other geomorphic surfaces

Cosmogenic exposure dating involves using the concentration of cosmogenic isotopes (e.g. ^{10}Be) within moraine boulders to determine the time the rock has been exposed to the surface. The isotope ^{10}Be forms at a known rate (~6 atoms/g/yr @ sea level) from the interaction of cosmic particles with quartz in rocks at the Earth's surface (Lal, 1991). Cosmic rays, however, decay exponentially with depth, and thus ^{10}Be production is negligible a few meters below the Earth's surface. Furthermore, ^{10}Be is radiogenic with a half-life of ~1.3×10^6 years, and thus is not present in buried rocks more than a few million years old. If we assume that moraine boulders have been eroded by the glacier from some small (>2 m) depth, then the boulders should contain no ^{10}Be when they are deposited by the glacier, and the concentration of ^{10}Be can therefore be used to infer surface exposure age of clasts and the moraine (see equation below).

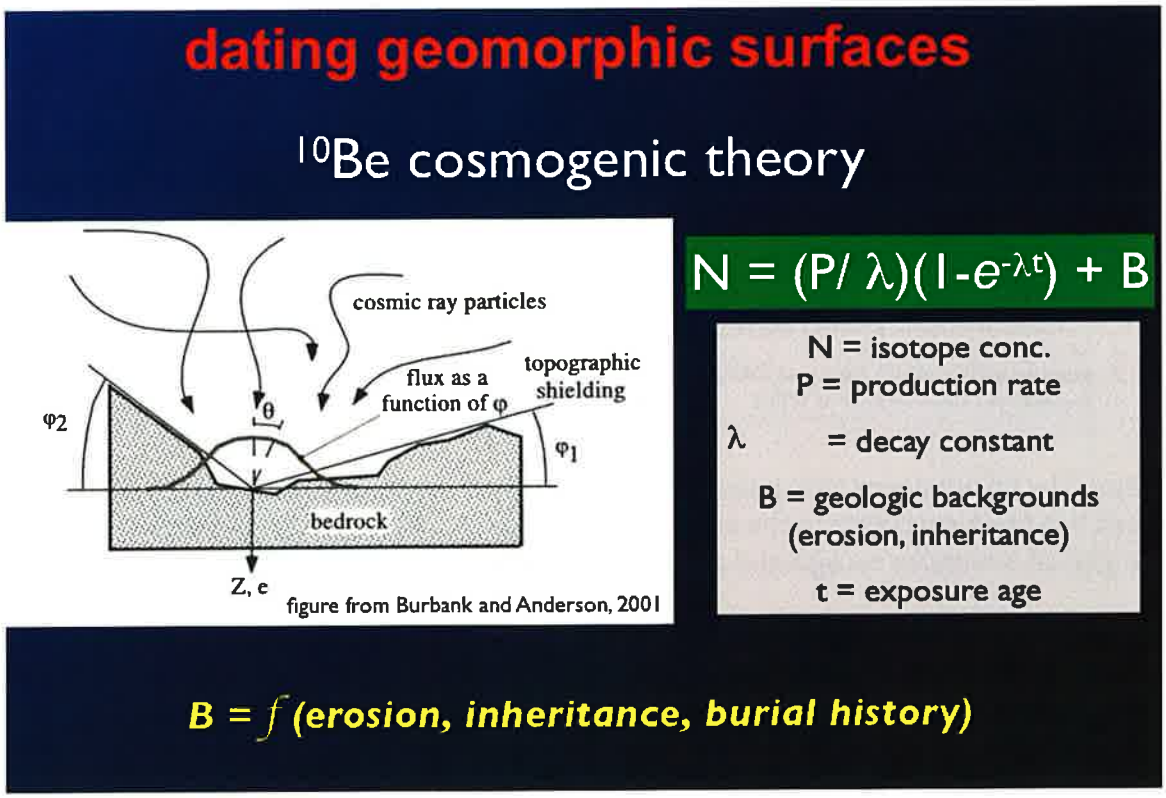

Sierra Nevada Glacial Advances (Gillespie and Zehfuss, 2004)

Table 1. Glaciations recognised in the Sierra Nevada, their ages and east-side ELAs relative to Tioga and interpolated to 37°

Glaciation	Mean age, ka[a]	ΔELA, m[b]	Age References
Matthes (Little Ice Age)	0.6- 0.1 [c]	480±25	Wood (1977); Stine (1994)
Recess Peak	14.2-13.1 [c]	335±20	Clark (1997)
Tioga (retreat)	15-14	125±30	James *et al.* (2002); Clark & Gillespie (1997)
Tioga (start)	21-20 [c]	0	Clark *et al.* (2003)
	<25 [c]	0	Bursik & Gillespie (1993)
Tioga ('Tioga 2-4')	25-16	0	Phillips *et al.* (1996)[d]
Tenaya ('Tioga 1')	31	-45±15	Phillips *et al.* (1996)[d]; Benson *et al.* (1996)
	32 [c]		Bursik & Gillespie (1993)
Tahoe II[††]	50-42	-95±10	Phillips *et al.* (1996)
Tahoe I[††]	?	*c.* -100?	
Casa Diablo	126-62	?	Bailey *et al.* (1976)
pre-Tahoe (Bloody Canyon)[e]	220-140	?	Phillips *et al.* (1990), discussed in Gillespie *et al.* (2003)
Mono Basin	80-60	-195±50	Phillips *et al.* (1990)[d]
Walker Creek[e]	*c.* 550	?	Clark (1968); Sarna-Wojcicki, quoted in Gillespie *et al.* (2003)
Sherwin	*c.* 820	*c.* -200	Sharp (1968); Birkeland *et al.* (1980), Nishiizumi *et al.* (1989)
Lower Rock Creek	*c.* 920	?	Sharp (1968); Birkeland *et al.* (1980)
McGee	2,700-1,500	?	Huber (1981); Dalrymple (1963, 1964)

a. Ages are shown as ranges or approximate values. Uncertainties may be found in text and/or references.
b. Elevation differences are relative to the lowest Tioga ELA (*c.* 3040 ± 150 m) and interpolated to 37°N (Gillespie, 1991). Uncertainties are ± 1 δ and are random and do not include the systematic uncertainties of *c.* 150m. Accuracy depends critically on assignment of moraines to the correct glaciation. Regression was done on ≤70 glaciated drainages.
c. 10^3 cal yr B.P.
d. Revised (see discussions in James *et al.*, 2002, and Phillips *et al.*, 2001).
e. Nomenclature from Gillespie *et al.* (2003)

Major Glacial advances that have been recognized in the Sierra Nevada. Most of this work has been complete to the south of Lake Tahoe. In the northern Sierra Nevada, the glacial advances recognized are ~76 ka, 49 ka, and 18.5 ka (James et al., 2002).

We will look at the lateral moraines near Sardine Lake and try to differentiate the different glacial advances that have occurred in this region.

References:

Gillespie, A. R., Zehfuss, P. H., Ehlers, J., and Gibbard, P. L., 2004, Glaciations of the Sierra Nevada, California, USA, Developments in Quaternary Sciences, Volume Volume 2, Part B, Elsevier, p. 51-62.

James, L. A., Harbor, J., Fabel, D., Dahms, D., and Elmore, D., 2002, Late Pleistocene Glaciations in the Northwestern Sierra Nevada, California: Quaternary Research, v. 57, no. 3, p. 409-419.

The basement rocks exposed in the Lakes Basin belong are part of a Paleozoic island arc that likely formed not far from the North American continental margin at that time.

By Richard Cardwell (from a field trip with Elwood Brooks, Cal State East Bay):
The Late Devonian – Early Mississippian island arc complex is represented by three formations of volcanic assemblages. The Sierra Buttes is the oldest (Late Devonian), followed by the Elwell Formation (Late Devonian) and the Taylor Fm (Late Devonian – Early Mississippian). These are overlain by chert of the Miss – Penn age Peale Fm. The entire package is known as the Taylorsville sequence.

All of the formations appear to be deposited under subaqueous, marine conditions at a depth of approximately one km of water. There is very little indication of subaerial deposition. The Late Devonian – Early Mississippian age of the Taylorsville sequence is established by conodonts and goniatites. The entire sequence was metamorphosed multiple times. In this area, most rocks are lower greenschist facies, although some rocks containing prehnite-actinolite facies also occur.

Stop 3-2: Lunch in Graeagle, CA

Stop 3-3: Fallen Leaf Lake, SW Lake Tahoe. Look at newly-recognized fault scarps in the Lake Tahoe basin (active normal faults).

A high-resolution seismic CHIRP investigation of active normal faulting across Lake Tahoe Basin, California-Nevada

J. Dingler[1,§], G. Kent[1], N. Driscoll[1], J. Babcock[1], A. Harding[1], G. Seitz[2], B. Karlin[3], and C. Goldman[4]
[1]*Scripps Institution of Oceanography, University of California, San Diego, La Jolla, California 92093, USA*
[2]*Department of Geological Sciences, San Diego State University, San Diego, California 92182, USA*
[3]*Department of Geological Sciences, University of Nevada, Reno, Nevada 89557, USA*
[4]*Department of Environmental Science and Policy, University of California, Davis, California 95616, USA*

ABSTRACT

We measured extension rates across Lake Tahoe Basin for the last 60 ka, based on measured displacement of offset marker surfaces across three active faults beneath Lake Tahoe. Seismic chirp imaging with submeter accuracy, together with detailed multibeam and light detection and ranging (LIDAR)–derived bathymetry, was used to measure fault offset, thickness of earthquake-derived colluvial wedges, depth of wave-cut paleoterraces, and other geomorphic features. An analysis of these features provides refined estimates of extension rates and new information on Holocene faulting, and places Tahoe Basin deformation into the larger context of Walker Lane and Basin and Range tectonics. Measured offset marker surfaces include submerged wave-cut paleoterraces of Tioga age (19.2 ± 1.8 ka), McKinney Bay slide deposits (ca. 60 ka), and a winnowed boulder surface of Tahoe age (ca. 62 ka). Estimated vertical offset rates across submerged geomorphic surfaces are 0.43–0.81 mm/a for the West Tahoe fault, 0.35–0.60 mm/a for the Stateline–North Tahoe fault, and 0.12–0.30 mm/a for the Incline Village fault. These offset rates indicate a combined east-west extension rate across Lake Tahoe Basin, assuming 60° fault dips, of 0.52–0.99 mm/a. This estimate, when combined with the Genoa fault-slip rate, yields an extension rate consistent with the magnitude of the extension deficit across Carson Valley and Lake Tahoe Basin derived from global positioning system (GPS) velocities. The Stateline–North Tahoe, Incline Village, and West Tahoe faults all show evidence for individual Holocene earthquake events as recorded by either colluvial wedge deposits or offset fan-delta stratigraphy.

INTRODUCTION

This paper updates extension rates in Lake Tahoe Basin through the measurement of fault offset, thicknesses of earthquake-derived colluvial wedges, depths of wave-cut paleoterraces, and other geomorphic features. These results are important for placing Holocene to late Pleistocene deformation in the context of the present strain field as measured by global positioning system (GPS), and they may permit a reassessment of slip budgets for the region. The changing stress field in the Walker Lane region during the Pliocene and Pleistocene (Zoback, 1989; Wesnousky and Jones, 1994; Bellier and Zoback, 1995) is still a matter of debate, and it cannot be completely resolved by GPS studies alone. As slip rates for each of the active faults in the basin are refined, the residual difference between GPS and fault slip will provide new insight into strain partitioning and the potential displacement deficit that may exist between GPS and fault-slip data in Lake Tahoe Basin and Carson Valley. This analysis, in turn, will provide greater understanding of strain partitioning and extension in high dextral shear regions, and the role of off-fault diffuse strain.

High-resolution light detection and ranging (LIDAR) and multibeam mapping conducted in 1998 (Gardner et al., 1998, 2000) combined with high-resolution seismic chirp imaging (Kent et al., 2005) provide a tool for measuring deformation across faults in Lake Tahoe Basin. These results can be related to the overall strain field through comparison with modern GPS measurements (Hammond and Thatcher, 2004). Our onshore-offshore study employed high-resolution seismic CHIRP imaging, lake-bottom sediment cores, and onshore paleoseismic trenching, which together provide new constraints on deformation within Walker Lane at an unprecedented scale (Fig. 1). These data have the resolution required to accurately measure Holocene and late Pleistocene fault displacement and deformation. While previous seismic studies have revealed important structural features in the lake (Hyne et al., 1972), they lack the resolution needed to define fault offsets of late Pleistocene and Holocene sequences at a resolution approaching onshore paleoseismic measurements. Throughout this paper, the term "active fault" refers to a fault that has exhibited deformation during the Holocene. The CHIRP profiles acquired between 1999 and 2006 allow us to examine the surface geomorphology and subsurface expression of three active faults beneath Lake Tahoe (i.e., the West Tahoe–Dollar Point, Stateline–North Tahoe, and Incline Village faults), as well as other important tectonic offset markers and geomorphic features.

Seismic CHIRP profiles also provide independent evidence of faults mapped into, or striking toward the lake, indicating whether they are actual faults or misidentified glacial or fluvial features. Active faults extending into the lake should show subsurface deformation offshore. A comparison of CHIRP profiles to previously published articles and geologic maps, such as the official State of California geology map for the Lake Tahoe region (Saucedo, 2005), allows us to independently confirm or refute the existence of offshore faults. For example, over 25 km of seismic CHIRP data in Emerald Bay show that the mapped Tahoe–Sierra frontal fault zone, as purported by Schweickert et al. (2004), does not have an associated offshore expression, even though the fault is claimed to be active, offsetting moraines on both sides of Emerald Bay. Based on the distribution of CHIRP profiles throughout Lake Tahoe, we are able to characterize active faulting beneath most portions of the lake (Fig. 2).

§Current address: BP America, Inc., Houston, TX 77079, USA; E-mail: jeffrey.dingler@bp.com.

GSA Bulletin; July/August 2009; v. 121; no. 7/8; p. 1089–1107; doi: 10.1130/B26244.1; 17 figures; 1 table.

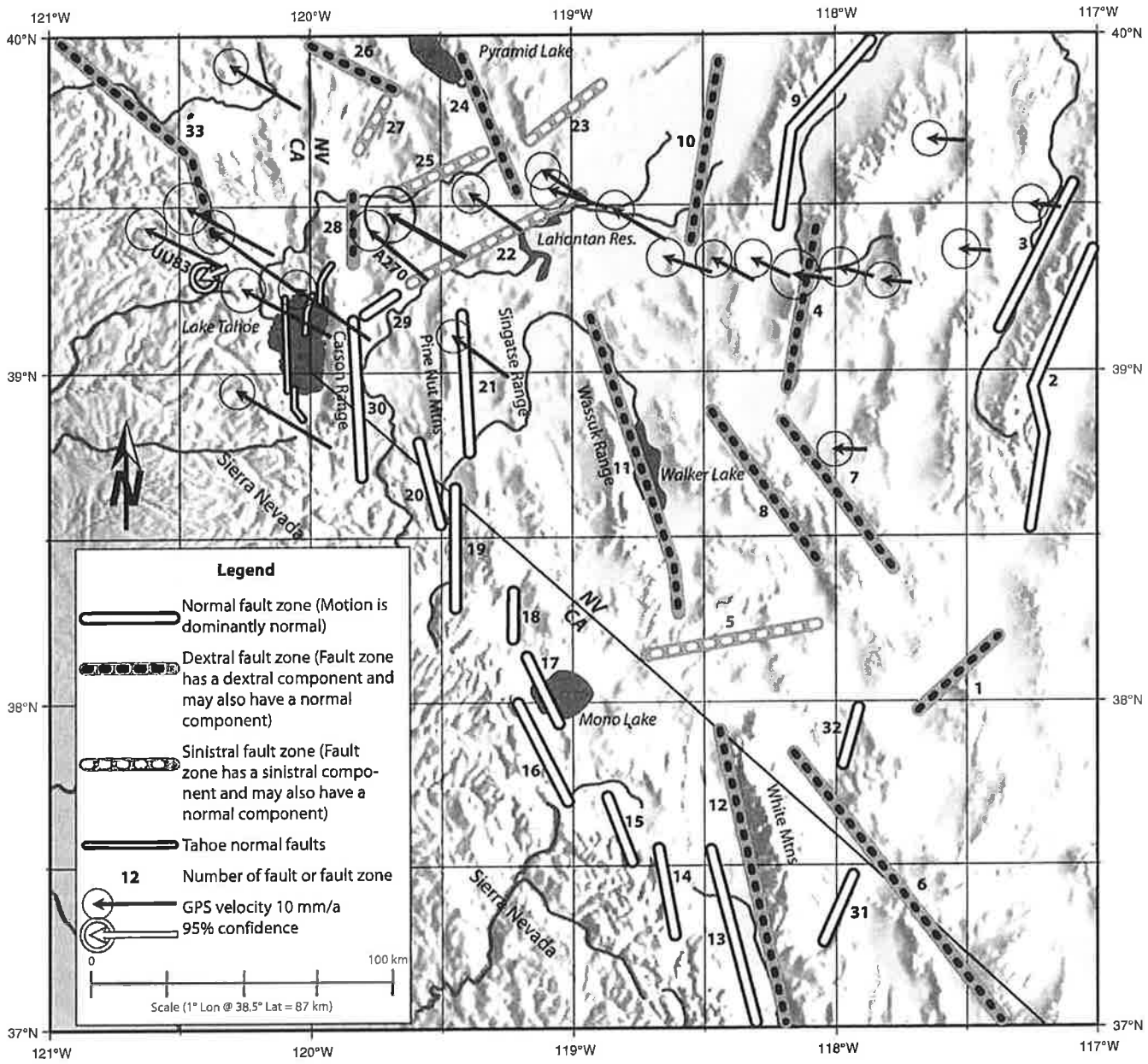

Figure 1. Map of the central and northern Walker Lane showing major fault zones and global positioning system (GPS) velocities (after Hammond and Thatcher, 2004; Table 1). Normal and dextral faults shown outside Lake Tahoe have deformation rates >0.2 mm/a (USGS, 2005). Sinistral faults shown have deformation rates <0.2 mm/a. The white on black GPS arrow to the west of Lake Tahoe shows a calculated relative velocity difference of 2.7 ± 0.9 mm/a between stations UU83 and A270, which are located to the north-northwest of Lake Tahoe and on the east side of the Carson Valley, respectively. At the eastern margin of Walker Lane, normal faults strike north-northeast and include the Central Nevada seismic belt. Dextral faults dominate away from the margin of the Sierra Nevada microplate and strike north-northwest. Sinistral faults strike northeast and are primarily located perpendicular to dextral faults in Northern Walker Lane. Individual fault segments (USGS, 2005) have been combined to form one approximate fault trace for each fault zone. 1—Lone Mountain fault zone; 2—Toiyabe Range fault zone; 3—Western Toiyabe Range fault zone; 4—Fairview fault zone; 5—region with numerous unnamed sinistral faults; 6—Fish Lake Valley fault zone; 7—Bettles Wells–Petrified Springs fault zone; 8—Benton Springs fault; 9—Dixie Valley fault zone; 10—Rainbow Mountain fault zone; 11—Wassuk Range fault zone; 12—White Mountains fault zone; 13—Owens Valley fault zone; 14—Round Valley fault; 15—Hilton Creek fault; 16—Hartley Springs–Silver Lake faults; 17—Mono Lake fault; 18—Robinson Creek fault; 19—West Walker River fault; 20—Antelope Valley fault; 21—Smith Valley fault zone; 22—Carson lineament; 23—unnamed faults SE of Truckee Range; 24—Pyramid Lake fault zone; 25—Olinghouse fault; 26—Honey Lake fault zone; 27—unnamed fault west of Hungry Valley; 28—Mount Rose fault zone; 29—Kings Canyon fault; 30—Genoa fault; 31—Deep Springs fault; 32—Emigrant Peak fault zone; 33—Mohawk Valley fault.

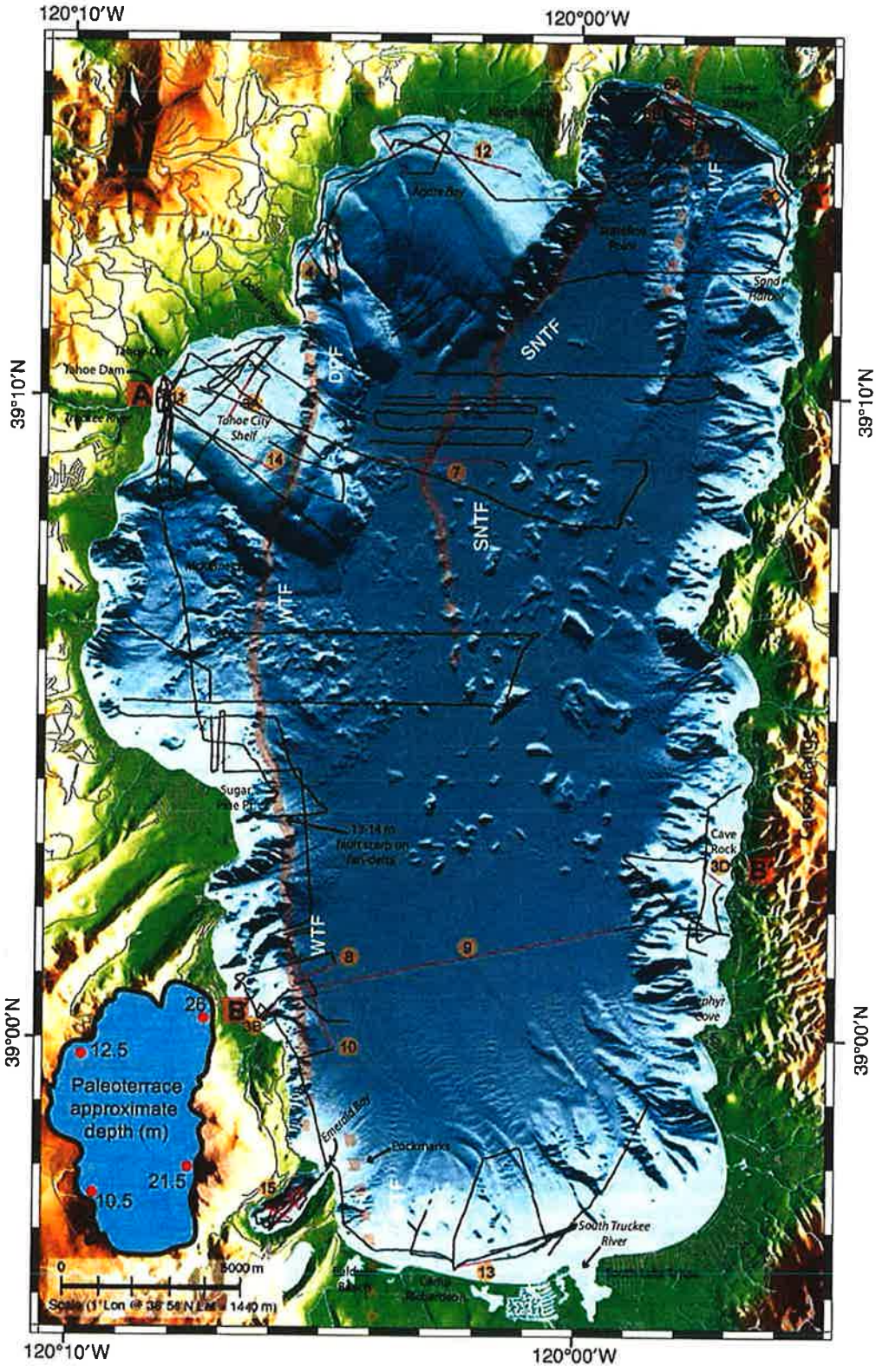

Figure 2. Combined bathymetry and topography map of Lake Tahoe highlighting active faults and chirp profiles. Active faults are represented by semi-transparent thick red lines, dashed where fault locations are inferred; WTF—West Tahoe fault; DPF—Dollar Point fault; SNTF—Stateline–North Tahoe fault; IVF—Incline Village fault. Thin brown lines delineate CHIRP profiles and are labeled with figure numbers for profiles presented in this paper. Thin, gray bathymetric contours are in 50 m intervals. The lake sill, at the Lake Tahoe Dam at the mouth of the Truckee River, is at ~1899 m, and the deepest point is ~1300 m, corresponding to a maximum lake depth of ~499 m. Bathymetry is a combination of SHOALS LIDAR (light detection and ranging) and EM1000 multibeam bathymetric surveys (Gardner et al., 1998, 2000), with a horizontal resolution of 10 m. Topography is interpolated from 10 m U.S. Geological Survey digital elevation model (DEM). Small inset of Lake Tahoe outline displays the approximate depth of the wave-cut paleoterrace at four locations throughout the lake. The paleoterrace increases in depth from west to east and from south to north.

a number of predefined pulses in the frequency range from 500 Hz to 16 kHz. The CHIRP profiles presented in this paper predominantly use a 1–5.5 kHz pulse with a 10 ms duration, a 1–5.5 kHz pulse with 30 ms duration, or a 1–6 kHz pulse with a 50 ms duration. The SIOSEIS processing package developed by Paul Henkart at Scripps Institution of Oceanography was used to process the data. Processing included the following steps: data conversion to standard SEGY, manual or automatic water-bottom picking, trace mix, amplitude gain starting at the water-bottom, and display. Two-way traveltimes were converted to depth assuming a water velocity of 1500 m/s. This conversion provides an accurate representation of the lake bottom and a minimum bound on sediment thicknesses.

RESULTS

Survey Overview

We acquired over 400 line kilometers of CHIRP data in Lake Tahoe both on- and off-fault, covering most of the geographical regions of the lake, including nearshore and deep-water environments. The on-fault profiling imaged the offset of individual sediment layers or sequences across a fault, while the off-fault profiles allowed us to compare the relative depth of the ca. 19.2 ka wave-cut paleoterrace around Lake Tahoe. We also identified other geomorphic features, such as infilled river channels, submarine landslides, and clinoform sequences that provided additional information about the tectonic activity of the basin. Here, we will present the observed stratigraphy in Lake Tahoe from youngest to oldest, and then we will discuss vertical offset across the fault systems from west to east.

LAKE TAHOE STRATIGRAPHY

Wave-Cut Paleoterrace (W_1)

The paleoterrace (W_1) is a shallow, relatively flat surface observed in the high-resolution bathymetry (Fig. 2), and it has been dated at 19.2 ± 1.8 ka near Cave Rock on the east shore (Kent et al., 2005). In CHIRP profiles, the paleoterrace is evident as a well-defined unconformity when mantled with sediment, or as a truncation surface when no sediment mantle is present. Varying amounts of sediment mantle this surface. For example, in many locations, prograding deltas or clinoforms extend out onto the paleoterrace surface and infill accommodation space created by a rise in lake level and/or tectonic subsidence of the surface since its formation (Figs. 3, 4, 5, and 6). Where buried, the paleoterrace has a similar flat appearance in CHIRP profiles.

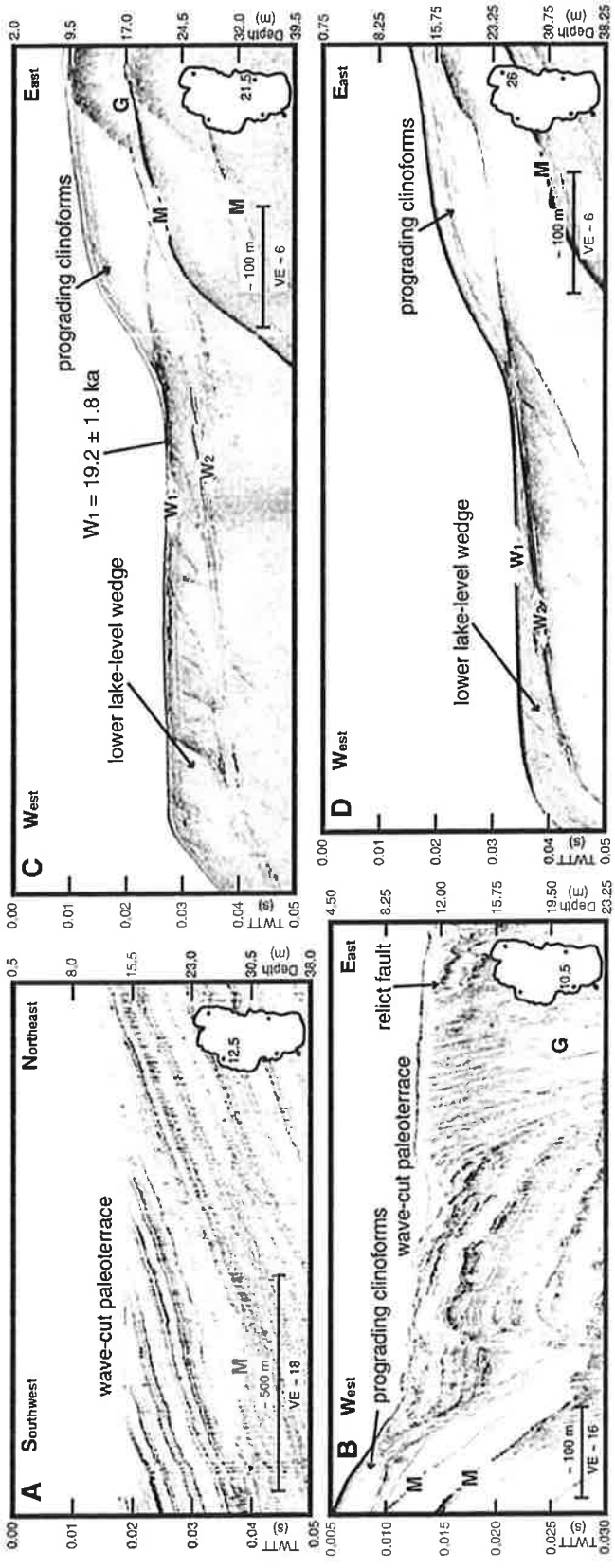

Figure 3. Chirp profiles crossing the ca. 19.2 ka wave-cut paleoterrace along the east and west shores of Lake Tahoe. The approximate depth of the wave-cut paleoterrace in meters is indicated next to the location of the current profile in the inset Lake Tahoe outline. The location of the other three profiles is marked with a dot, but no depth. (A) Profile across the Tahoe Shelf. Dipping reflectors are truncated in this profile. The depth of the paleoterrace is 12.5 ± 2.0 m. (B) Profile offshore of Rubicon. The paleoterrace is at a depth of 10.5 ± 0.5 m. Prograding clinoforms are building out onto the terrace from the west, and they unconformably overlie the paleoterrace. A relict fault is evident to the east, but it does not offset the surface of the paleoterrace. (C) Profile offshore Cave Rock. Two wave-cut surfaces are evident at 21.5 ± 0.5 m (W_1) and 28.5 ± 2.0 m (W_2). W_1 has an age of 19.2 ± 1.8 ka. (D) Profile offshore Hidden Beach, which shows the same wave-cut surfaces and prograding clinoforms as C, except W_1 is at a depth of 26.0 ± 1.0 m. TWTT—(two-way traveltime; VE—vertical exaggeration; M—water-bottom multiple; G—CHIRP ghost water-bottom multiple.

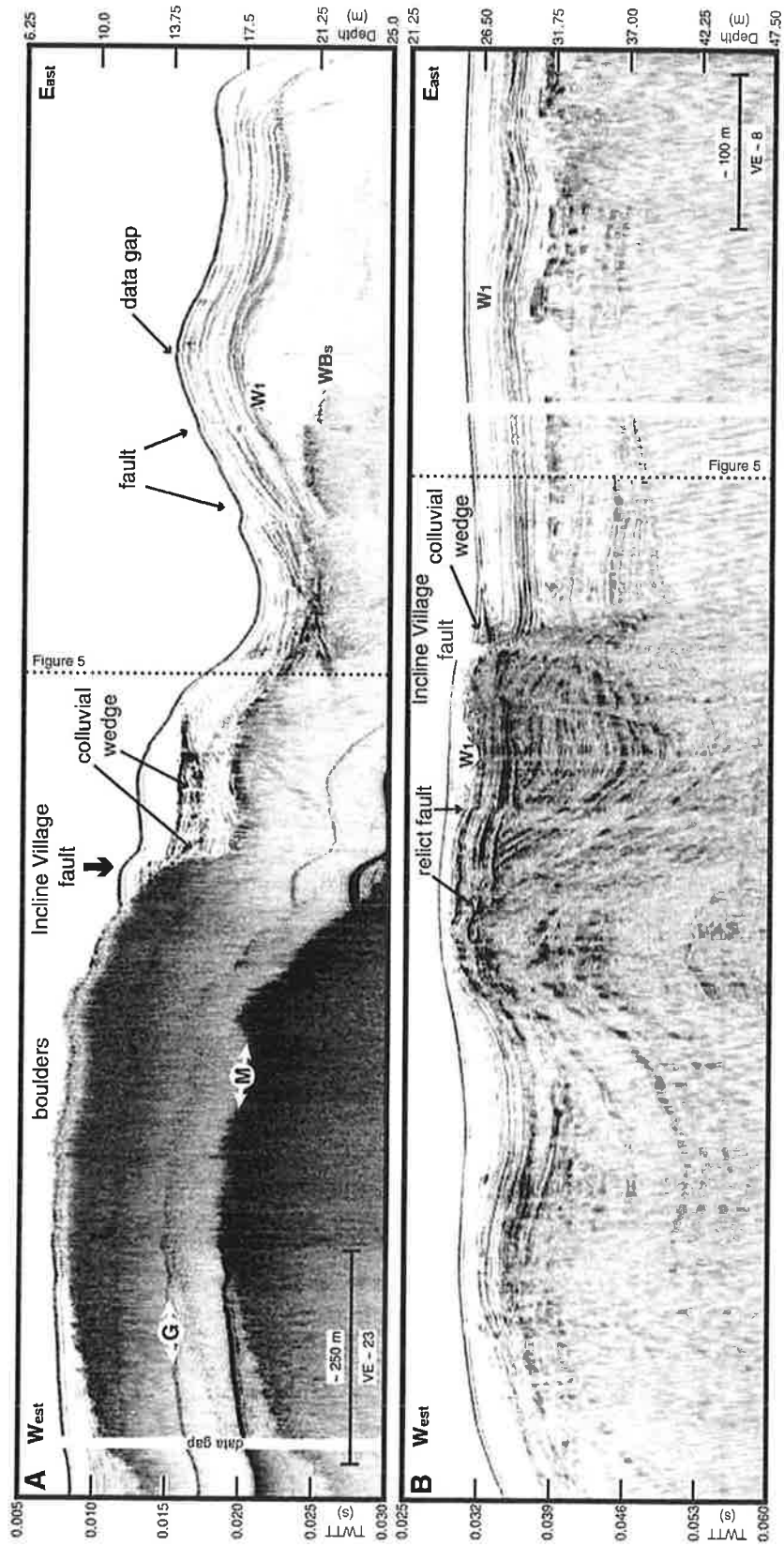

Figure 6. Chirp profiles across the Incline Village fault. (A) Shallower of the two fault-crossing profiles. The west side of the profile shows an acoustically opaque lake-bottom reflector with an extremely rough surface. This surface, imaged by remotely operated vehicle (ROV), is a boulder surface that has been winnowed (WBs) and was probably deposited during the Tahoe glaciation, ca. 62 ka. The WBs is offset ~14 m across the Incline Village fault at this location. Two colluvial wedges are evidence for large normal faulting events. (B) Deeper of the two fault-crossing profiles. Surface morphology shows an ~1-m-high fault scarp that offsets bedding layers for almost 20 m beneath the surface. W_1 is the ca. 19.2 ka paleoterrace, which is offset 3.0–3.5 m across the fault. The colluvial wedge in the top few meters of sediment suggests vertical offset during the Holocene. To the west of the Incline Village fault, there is a zone of deformation that contains two relict faults that do not offset the top 1–2 m of sediment. Dashed vertical line indicates where CHIRP profile Figure 5, parallel to the fault trace, intersects this profile. TWTT—two-way traveltime; VE—vertical exaggeration; M—water-bottom multiple; G—CHIRP ghost water-bottom multiple.

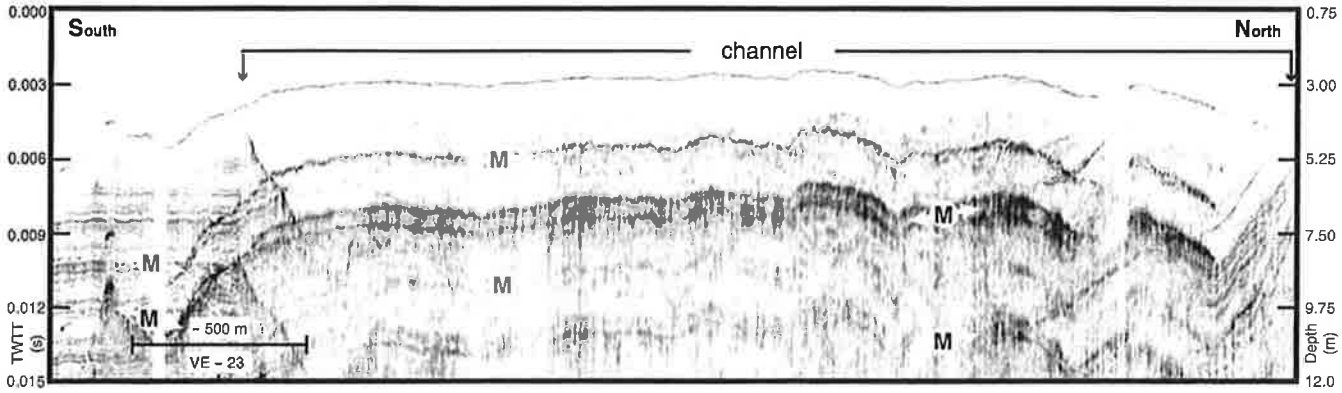

Figure 11. Chirp profile east of the Lake Tahoe Dam on the Tahoe City Shelf. Continuous layers are interrupted by a 9+-m-deep valley that is ~3.0 km wide. Another profile (Kent et al., 2005, their supplemental material) closer to the dam reveals a narrower, but well-imaged, 13-m-deep incised channel that is filled with unstratified fill. The southern side of the channel cuts through laminated layers, a result of catastrophic jökulhlaup failure farther down the Truckee River (Birkeland, 1964; Hyne et al., 1972). M—water-bottom multiple; TWTT—two-way traveltime; VE—vertical exaggeration.

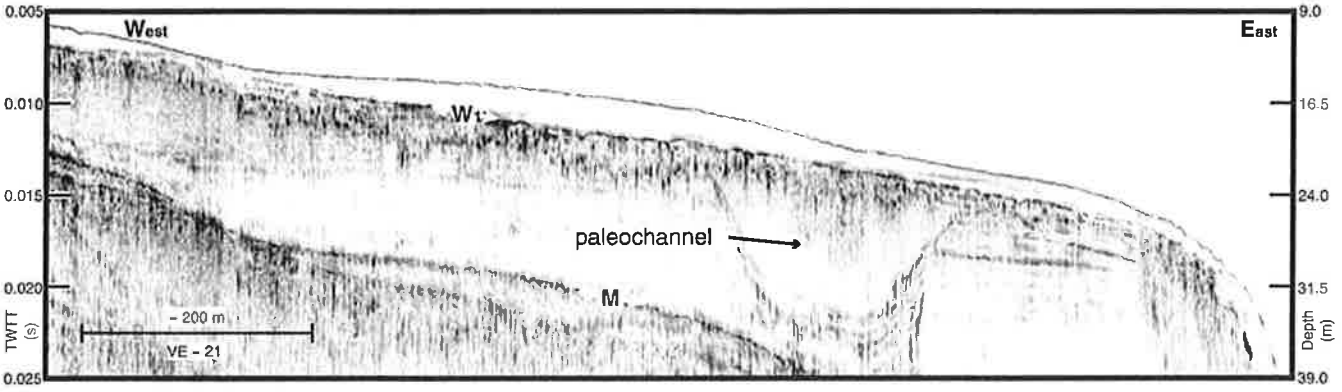

Figure 12. Chirp profile on the shelf offshore Camp Richardson. The ca. 19.2 ka paleoterrace is observed across the profile, but it is difficult to confidently identify a paleoshoreline depth because the profile is oblique to shore. The ~200-m-wide, ~15-m-deep paleochannel is truncated by the paleoterrace and may be an older channel associated with the Upper Truckee River. The truncation of the channel fill indicates that this channel is older than the paleoterrace, thus recording more down-to-the-east tectonic deformation. W_1—ca. 19.2 ka wave-cut paleoterrace; M—water-bottom multiple; TWTT—two-way traveltime; VE—vertical exaggeration.

Farther north along the southern edge of the Tahoe City Shelf, the scarp is ~100 m high, and there is possible slumping and faulting in the footwall block (Fig. 14). The scarp continues along the east edge of the Tahoe City Shelf to Dollar Point. The scarps exhibit similar relief to the north and south of the McKinney Bay slide, indicating that they are older than the slide itself and have been overprinted by the McKinney Bay slide.

Stateline–North Tahoe Fault

The Stateline–North Tahoe fault scarp exhibits multiple en echelon segments from offshore of Stateline Point to the middle of the lake, where the surface expression is obscured by the McKinney Bay slide deposits (Fig. 2). The fault trace changes strike with each eastward step for an overall ~30° strike change from south to north. The profile in Figure 7 is representative of the multiple east-west profiles collected across the fault, all of which image parallel-layered deposits conformably overlying McKinney Bay slide deposits. The western part of the profile also crosses a more recent slide deposit, which is clearly visible in the bathymetry off the eastern edge of the Tahoe City Shelf (Fig. 2). Six kilometers to the south, there is no evidence for offset across the Stateline–North Tahoe fault, but large slide blocks may obscure the fault trace. Continuing south (Fig. 9), where there are fewer slide blocks, there are no fault or fault-related features, suggesting that the Stateline–North Tahoe fault dies away in the center of Lake Tahoe (Fig. 2).

The post–McKinney Bay slide sediment sequence is offset by two parallel traces of the Stateline–North Tahoe fault (Fig. 7). Sedimentation rates for the upper 3 m of sediment are ~0.4 mm/a, based on radiocarbon dating of organic material recovered in a 3-m-long piston core from the hanging wall (Kent et al., 2005). The top of the McKinney Bay slide deposit is offset ~21 m across the two fault traces. The surface of the slide deposit has relief as a result of the catastrophic emplacement, so the 21 m estimate is based on the measured offset of the slide deposits directly adjacent to the fault. The postslide

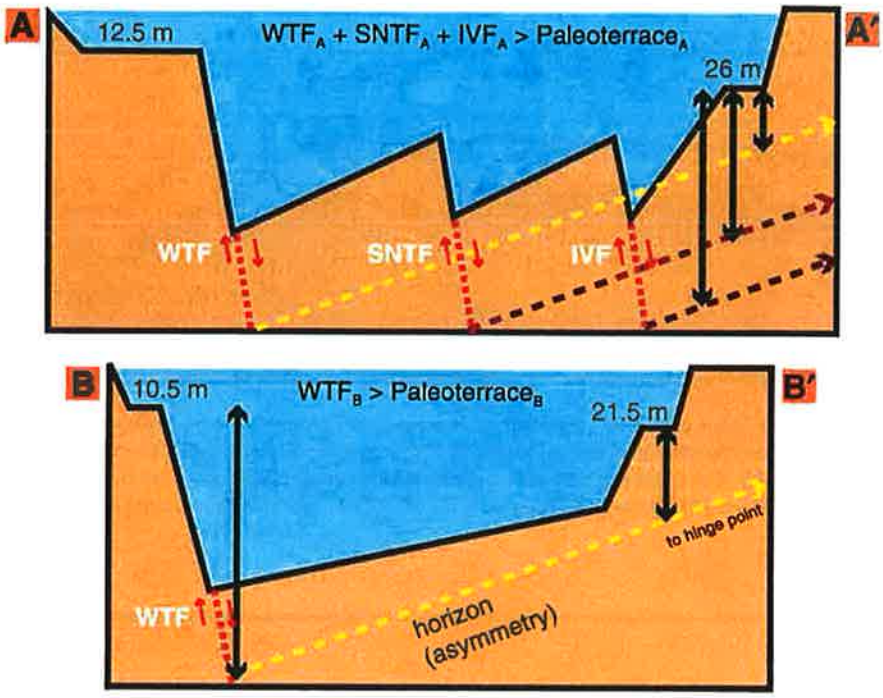

Figure 17. Schematic cross sections illustrate the approximate fault geometry in the northern (left, A–A′) and southern (right, B–B′) parts of the lake (see Fig. 2 for cross-section location). Green vertical arrows represent the relative vertical displacement measured across individual faults or on the wave-cut paleoterrace. The yellow dashed line is an idealized sedimentary horizon extending from the fault to the hinge point. Vertical deformation decreases with increasing distance away from the faults, so east-shore paleoterrace offset is a minimum estimate of fault offset. WTF—West Tahoe fault, SNTF—Stateline–North Tahoe fault, and IVF—Incline Village fault.

Subbottom deformation and faulting associated with the West Tahoe fault was imaged in a single CHIRP profile (Fig. 8). The probable location of the main fault trace is obscured by seismic diffractions in parallel CHIRP profiles to the north and south. Based on the strike of the West Tahoe fault where it crosses a fan delta to the north (Fig. 2), the actual West Tahoe fault trace is probably 100–300 west of the synthetic fault imaged in Figure 8. The inferred synthetic fault displays ~2 m of vertical offset 10 m below the surface, and the most recent offset reflectors display an offset of ~1.6 m at a depth of ~1.9 m below the surface. The synthetic fault offsets the ca. 8.5–12.0 ka slide mentioned earlier, so the most recent rupture event (MRE) must postdate this age. If sedimentation rates at this location, which is closer to the shelf, are higher than those at the core site used to determine the slide age, then the age of the last rupture event could be younger. Because this fault splay appears to be a synthetic fault, we cannot definitively determine whether this rupture event coincided with the last rupture event on the main trace of the fault.

The sedimentary structure observed in the cross-lake profile provides important constraints on basin architecture (Fig. 9). The CHIRP profiles confirm that sediment layers dip westward in conjunction with the overall dip of the lake floor (Figs. 9 and 17). This observation suggests that the West Tahoe fault is the controlling normal fault for the half-graben in the southern half of the lake. The ~0.1° slope of the lake floor along the cross-lake profile in the southern half of the lake allows a rough calculation of fault asymmetry and the approximate difference between an on-fault measurement on the West Tahoe fault and off-fault measurement on the east shore paleoterrace (Fig. 17). Assuming the lake floor was flat after the ca. 60 ka McKinney Bay slide, then the ~0.1° westward dip translates into increased offset on the West Tahoe fault (since 19.2 ka), compared to the ~11 m vertical offset measured on the east-shore paleoterrace. A comparison of the maximum slip rates for the paleoterrace and the fan-delta scarp from Table 1 also shows a higher maximum slip rate for the on-fault measurement at the fan delta. This is a rough measurement that could be refined in the future by deeper seismic imaging of the top of the McKinney Bay slide debris and more precise measurement of the change in dip of that surface. On the basis of these measurements, it is clear that vertical offset of the paleoterrace serves as an absolute minimum bound on fault offset.

Coalescing slide deposits from adjacent fan deltas indicate that some slides or other mass-wasting events may be earthquake triggered, because their initiation points are spatially separated, but the coalescing deposits indicate that they are concomitant. Additional CHIRP profiles and associated sediment cores will help constrain the origin and timing of the different slides. Sediment cores throughout the lake record turbidite sequences that may be related to these and other earthquake-triggered mass-wasting events.

Incline Village Fault

On the Incline Village fault, the vertical deformation rate is 0.18–0.30 mm/a since the formation of the winnowed boulder surface (WBs) ca. 62 ka, based on the 13–14 m vertical offset (Fig. 17). The estimated vertical deformation rate includes ±10% measurement error, +20% due to increased sediment velocity, and ±10% for error in dating of the winnowed boulder surface. The western of the two relict faults does not offset an older truncation surface, while the eastern relict fault offsets this surface, but not the ca. 19.2 ka paleoterrace (Fig. 6B). Though speculative, such an offset pattern suggests that the fault rupture has migrated eastward through time, which may record the long-term regional deformation that is measured by a slight counterclockwise rotation of GPS velocities (Hammond and Thatcher, 2004) across Carson Valley and Lake Tahoe Basin (Fig. 1, white arrow).

The second wave-cut surface, W_2, imaged beneath the ca. 19.2 ka paleoterrace in the two CHIRP profiles on the east shore would provide additional constraints on vertical deformation if accurate dates were available (Figs. 3C and 3D). Extrapolation of sedimentation rates based on the Vibracores in the vicinity of Cave Rock (Kent et al., 2005) is not feasible because the sedimentation rate is extremely variable due to changing lake levels. Deeper penetrating sediment cores and an improved lake-level chronology are needed to accurately date this surface.

The ca. 19.2 ka paleoterrace surface is offset by ~3.0–3.5 m across the Incline Village fault, which corresponds to a vertical deformation rate of 0.12–0.23 mm/a. The estimated vertical deformation rate includes ±10% measurement error, +20% due to increased sediment velocity,

Airborne LiDAR analysis and geochronology of faulted glacial moraines in the Tahoe-Sierra frontal fault zone reveal substantial seismic hazards in the Lake Tahoe region, California-Nevada, USA

James F. Howle[1,†], Gerald W. Bawden[2,†], Richard A. Schweickert[3,†], Robert C. Finkel[4,†], Lewis E. Hunter[5,†], Ronn S. Rose[5,†], and Brent von Twistern[6,†]

[1]*U.S. Geological Survey, P.O. Box 1360, Carnelian Bay, California 96140, USA*
[2]*U.S. Geological Survey, 3020 State University Drive East, Modoc Hall, Suite 4004, Sacramento, California 95819, USA*
[3]*University of Nevada, Reno, Department of Geological Sciences, 1900 Greensburg Circle, Reno, Nevada 89509, USA*
[4]*University of California, Berkeley, Earth and Planetary Science Department, 371 McCone Hall, Berkeley, California 94720, USA*
[5]*U.S. Army Corp of Engineers, 1325 J Street, Sacramento, California 95814, USA*
[6]*P.O. Box 5401, Incline Village, Nevada 89450, USA*

ABSTRACT

We integrated high-resolution bare-earth airborne light detection and ranging (LiDAR) imagery with field observations and modern geochronology to characterize the Tahoe-Sierra frontal fault zone, which forms the neotectonic boundary between the Sierra Nevada and the Basin and Range Province west of Lake Tahoe. The LiDAR imagery clearly delineates active normal faults that have displaced late Pleistocene glacial moraines and Holocene alluvium along 30 km of linear, right-stepping range front of the Tahoe-Sierra frontal fault zone. Herein, we illustrate and describe the tectonic geomorphology of faulted lateral moraines. We have developed new, three-dimensional modeling techniques that utilize the high-resolution LiDAR data to determine tectonic displacements of moraine crests and alluvium. The statistically robust displacement models combined with new ages of the displaced Tioga (20.8 ± 1.4 ka) and Tahoe (69.2 ± 4.8 ka; 73.2 ± 8.7 ka) moraines are used to estimate the minimum vertical separation rate at 17 sites along the Tahoe-Sierra frontal fault zone. Near the northern end of the study area, the minimum vertical separation rate is 1.5 ± 0.4 mm/yr, which represents a two- to threefold increase in estimates of seismic moment for the Lake Tahoe basin. From this study, we conclude that potential earthquake moment magnitudes (M_w) range from 6.3 ± 0.25 to 6.9 ± 0.25. A close spatial association of landslides and active faults suggests that landslides have been seismically triggered. Our study underscores that the Tahoe-Sierra frontal fault zone poses substantial seismic and landslide hazards.

INTRODUCTION

The Lake Tahoe basin, California and Nevada, is a tectonically active graben located between the Sierra Nevada microplate on the west and the Basin and Range Province to the east. The Tahoe-Sierra frontal fault zone, west of Lake Tahoe, was recognized over a century ago by early geologic investigators (Russell, 1885; Lindgren, 1896, 1897) from its topographic expression, but the locations of basin-bounding normal faults have remained elusive due to difficult access and dense vegetative cover in mountainous terrain. Schweickert et al. (2000, 2004) mapped the principal faults of the Tahoe-Sierra frontal fault zone along the steep, linear range front west of the lake. However, because complex tectonic geomorphology has been formed by normal faulting of glacial landforms and because dense vegetation obscures the morphology, the fault zone has remained controversial and was omitted from the state of California's seismic hazard risk assessment (UCERF2, 2007). This report documents the tectonic geomorphology of faulted moraines, establishes limiting ages of faulted late Pleistocene glacial and alluvial deposits, and quantifies the minimum vertical separation rate and extension rate along the Tahoe-Sierra frontal fault zone; it demonstrates that the Tahoe-Sierra frontal fault zone is an important seismic source for the region.

Bare-earth airborne light detection and ranging (LiDAR) imagery has revolutionized geomorphic mapping in densely vegetated, mountainous, and otherwise inaccessible terrain (Fig. 1). Recent studies of known fault zones (Hudnut et al., 2002; Frankel et al., 2007; Oskin et al., 2007; Prentice et al., 2009; Arrowsmith and Zielke, 2009; Zielke et al., 2010) and discoveries of previously unknown fault zones in densely vegetated terrain (Haugerud et al., 2003; Hunter et al., 2011) have exploited bare-earth airborne LiDAR imagery for fault-zone characterization. Utilizing new bare-earth LiDAR imagery (see GSA Data Repository for a discussion of the LiDAR data used in this study[1]) we have identified, visualized, and mapped faults within late Quaternary glacial, colluvial, and alluvial deposits and granitic bedrock along 30 km of range-front faults that comprise the central portion of the Tahoe-Sierra frontal fault zone (Fig. 2). We analyzed the LiDAR imagery using pseudo–sun angles, vertical exaggeration, and oblique perspectives and extracted profiles to facilitate geologic interpretation and to reveal (and in many cases confirm)

†E-mails: jfhowle@usgs.gov; gbawden@usgs.gov; rschweickert@gmail.com; rfinkel@berkeley.edu; lewis.e.hunter@usace.army.mil; ronn.s.rose@usace.army.mil; bvtwist@journeyaroundhappy.com.

[1]GSA Data Repository item 2012192, includes supplementary discussions of the airborne LiDAR data, late Pleistocene glacial deposits and stratigraphy, geochronology of Tioga and Tahoe deposits, Emerald Bay bathymetric data, mathematical modeling of planes and vectors, Root-Mean-Square error estimates, modeled tectonic displacements, DR Figures 1–16 and DR Tables 1–6, is available at http://www.geosociety.org/pubs/ft2012.htm or by request to editing@geosociety.org.

GSA Bulletin; July/August 2012; v. 124; no. 7/8; p. 1087–1101; doi:10.1130/B30598.1; 8 figures; 1 table; Data Repository item 2012192.

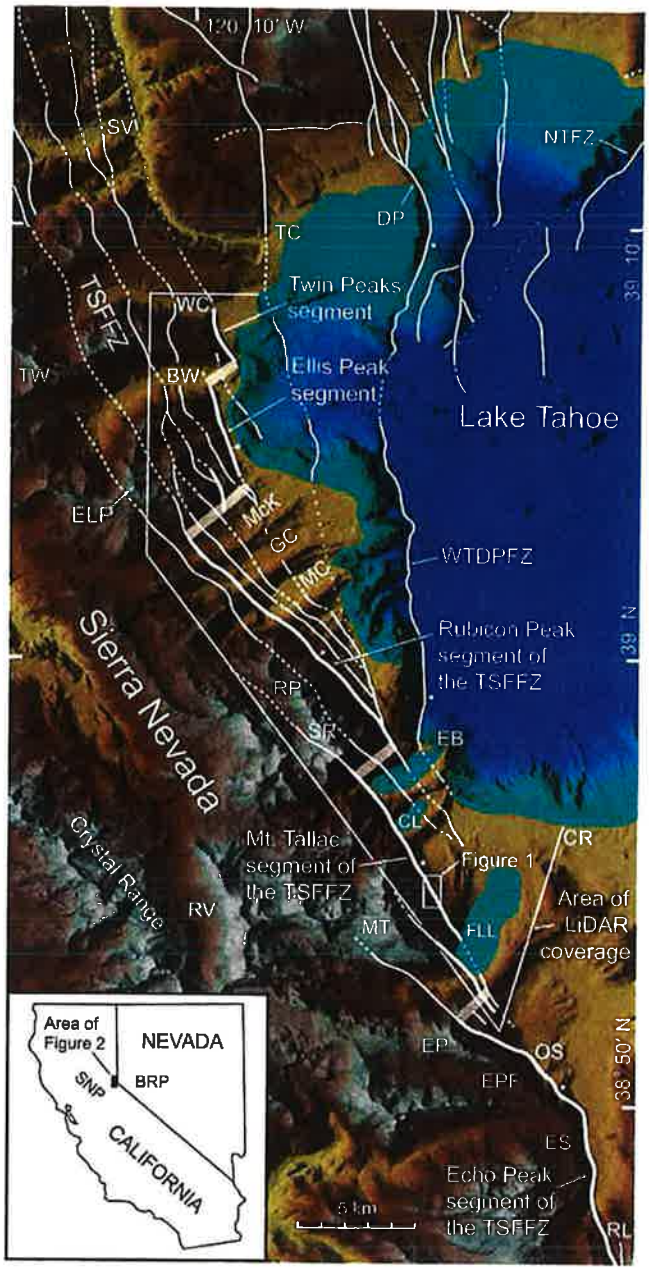

Figure 2. Shaded relief map of western part of the Lake Tahoe basin, California. Map shows area of airborne LiDAR coverage, mapped faults, and selected geographic locations discussed in text. Faults are dashed where approximately located, dotted where concealed, bar and ball on downthrown side. Heavier line weight shows principal range-front fault strands of the Tahoe-Sierra frontal fault zone (TSFFZ). Opaque white boxes indicate approximate segment boundaries and right steps in range front separating principal fault strands. Mapped faults are modified from Schweickert et al. (2000). BRP—Basin and Range Province; BW—Blackwood Creek; CL—Cascade Lake; CR—Camp Richardson; DP—Dollar Point; EB—Emerald Bay; ELP—Ellis Peak; EP—Echo Peak; EPF—Echo Peak fault; ES—Echo Summit; FLL—Fallen Leaf Lake; GC—General Creek; MC—Meeks Creek; McK—McKinney Creek; MT—Mt. Tallac; NTFZ—North Tahoe fault zone; OS—Osgood Swamp; RL—Round Lake; RP—Rubicon Peak; RV—Rockbound Valley; SNP—Sierra Nevada microplate; SR—Stony Ridge; SV—Squaw Valley; TC—Tahoe City, California; TW—Twin Peaks; WC—Ward Creek; WTDPFZ—West Tahoe–Dollar Point fault zone.

Limiting Ages of the Tioga Maximum Moraines

Our new TCN exposure age of 20.8 ± 1.4 ka for the largest and longest Tioga moraine (Tioga maximum) at Meeks Creek (see TCN discussion in GSA Data Repository and Data Repository Table DR1 [see footnote 1]) is consistent with radiocarbon age control at a site ~30 km southeast, where the Tioga maximum had previously been dated at ≥20.5 ± 0.6 ka (Clark et al., 2003). In the Bear River drainage, ~60 km northwest of Meeks Creek, the Tioga maximum occurred at 18.6 ± 1.2 ka (James et al., 2002). These data from the Lake Tahoe region indicate that the Tioga maximum advance occurred between ~ca. 19 and 21 ka, which correlates well with the Tioga 2 stage of Phillips et al., 2009 (see Table 1, this paper). In the central and southern Sierra Nevada, the Tioga maximum is correlated with the Tioga 1 stage between 25.2 ± 2.5 ka (Bursik and Gillespie, 1993) and 26.5 ± 1.7 ka (Phillips et al., 2009). In this study, we have considered the possibility that the highest Tioga moraines in other valleys between Fallen Leaf Lake and McKinney Creek, where we do not have site-specific chronology, may have been deposited during the older Tioga 1. Therefore, for calculation of tectonic slip rates along the Tahoe-Sierra frontal fault zone, we use the ≥20.5 ka age (Clark et al., 2003) as a minimum bound and the 26.5 ka age (Phillips et al., 2009) as a maximum bound and use the average value of 23.5 ± 3 ka as a broad and conservative estimate for the age of the Tioga maximum moraines.

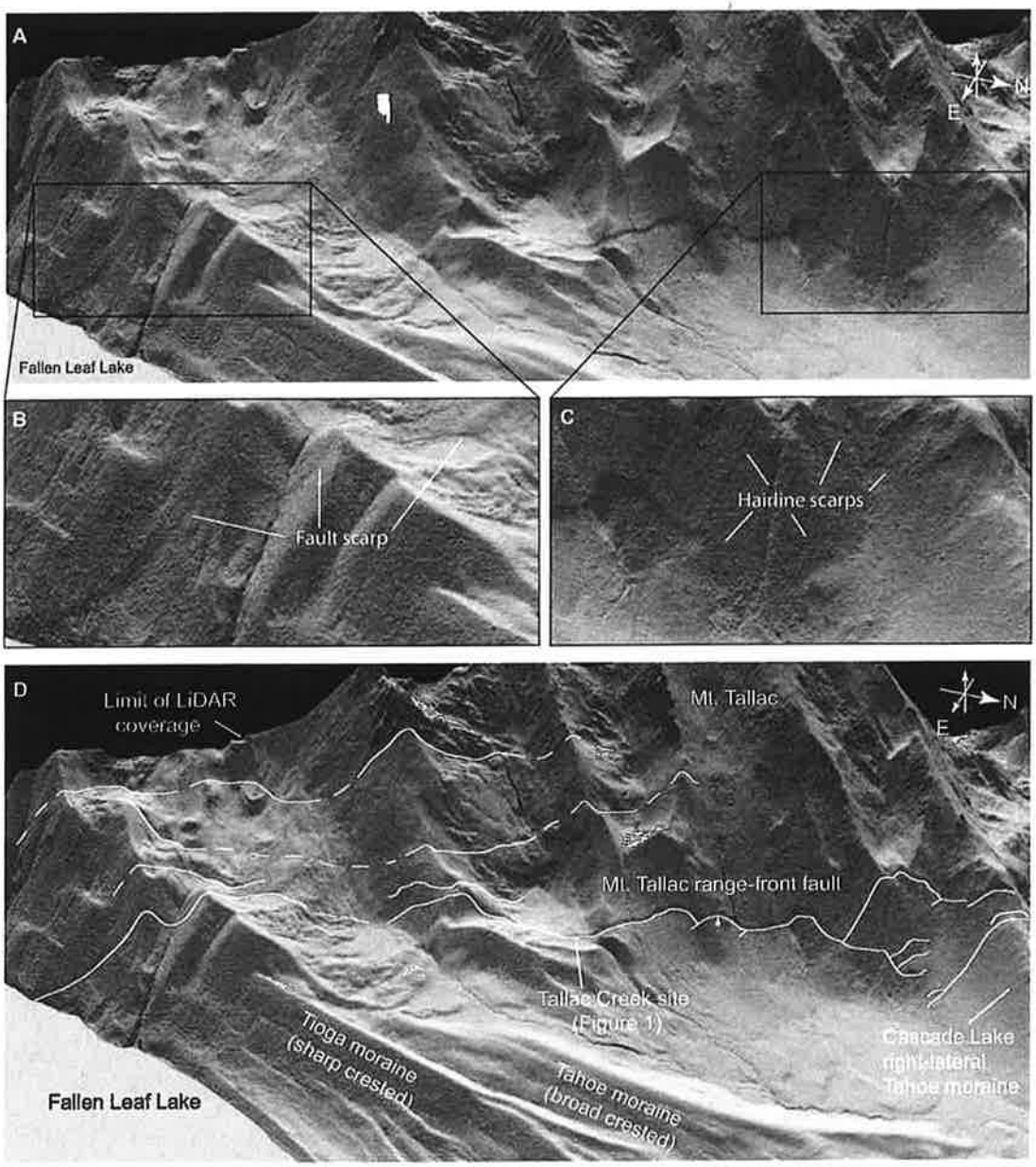

Figure 3. Oblique bare-earth LiDAR image of Mt. Tallac range-front fault. (A) View is to the west-southwest extending from Fallen Leaf Lake to the Cascade Lake right-lateral moraine, a horizontal distance of ~4.5 km along the base of the range front. Vertical exaggeration is 1.75. Hand icon shows illumination direction. (B) Detail of fault scarp above Fallen Leaf Lake. (C) Detail of diffuse ground-rupture traces and hairline scarps southeast of Cascade Lake. (D) Annotated view in A, showing the nearly continuous, 4.5-km-long range-front scarp of the Mt. Tallac fault, and selected geographic features. Faults are dashed where approximately located, bar and ball on downthrown side. Note the linear, evenly graded (unfaulted) Tioga and Tahoe moraines north of Fallen Leaf Lake. See Figure DR1 for geologic map of the Mt. Tallac range front (see text footnote 1).

data and modeled for vertical separation and extension (see Figs. DR3B and DR3C [see footnote 1]). We constructed these profiles, ranging from 69 to 159 m in length, by extracting a 2-m-wide swath of the LiDAR point cloud data and projecting the points into the vertical planes of the profiles (Fig. DR3 [see footnote 1]). This swath-sampling technique effectively integrates several closely spaced profiles from the point cloud into a single profile with greater data density. On the basis of 3-D modeling of fault planes in the study area (see Fig. DR4 [see footnote 1]), the Mohr-Coulomb failure criteria for normal faults (McCalpin, 1996), and field observations of dips of range-front faults in the Basin and Range Province (Slemmons, 1957; Bateman, 1965; Wallace, 1977; Clark et al., 1984), we modeled fault planes with dips

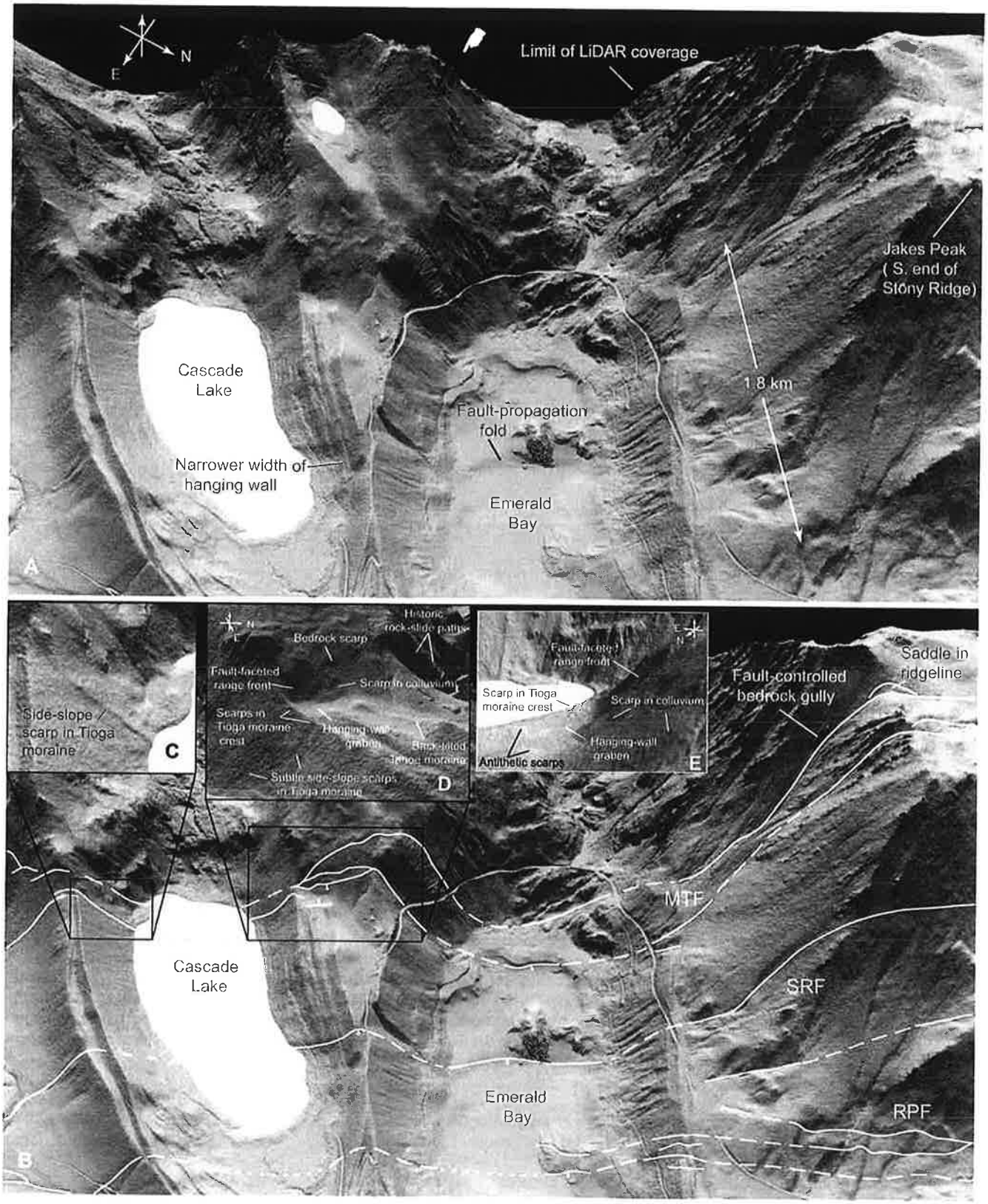

Figure 4.

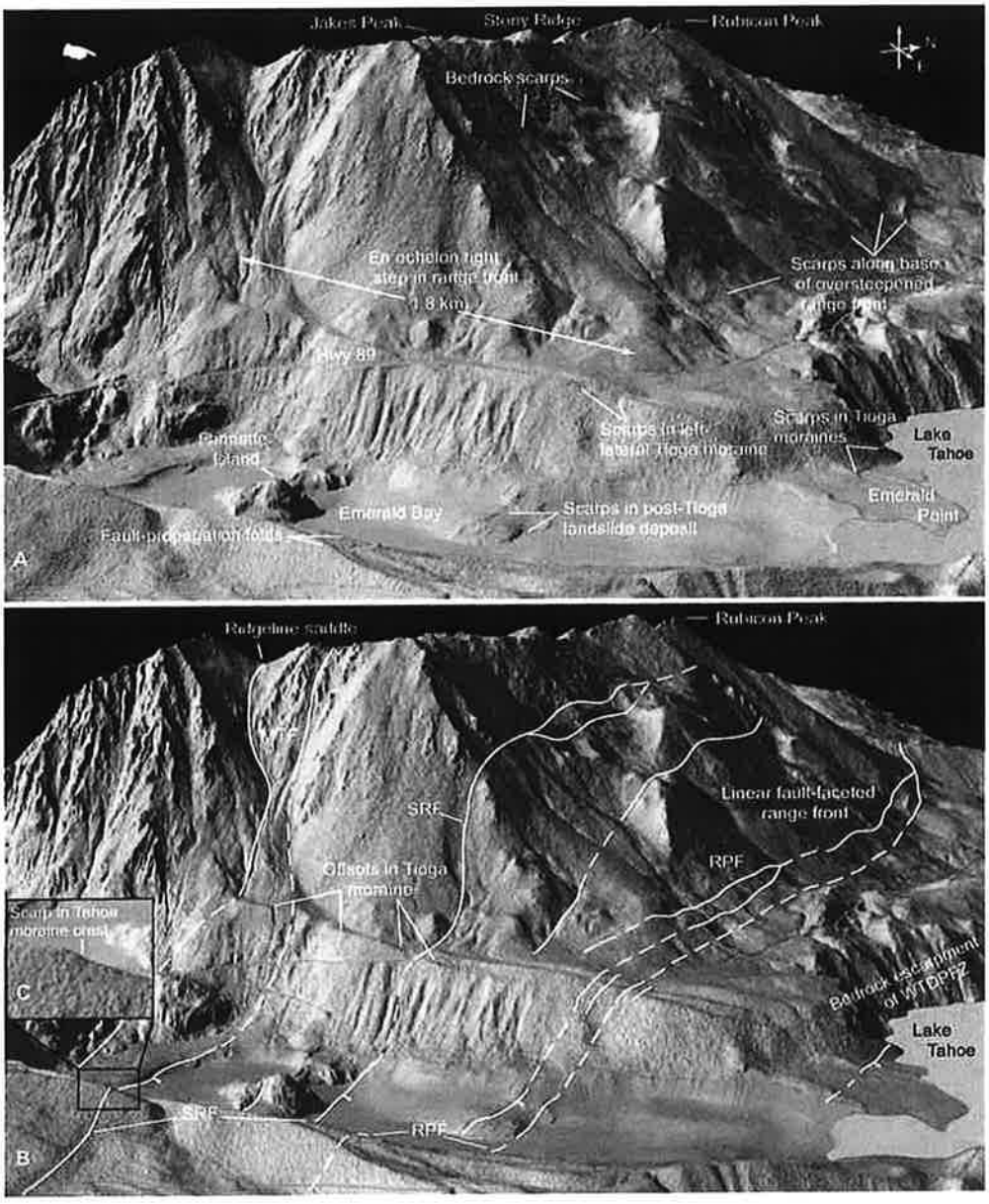

Figure 5. Oblique bare-earth LiDAR image of Stony Ridge and bathymetry of Emerald Bay. (A) View is to the west-northwest, showing en echelon right step in range front, linear fault-bounded range front north of Emerald Bay, tectonic geomorphology, and selected geographic features discussed in text. Hand icon shows illumination direction. Vertical exaggeration is 1.4. Distance across bottom of image is 2.4 km. (B) Faults discussed in text; dashed where approximately located, bar and ball on downthrown side. MTF—Mt. Tallac fault zone; RPF—Rubicon Peak fault zone; SRF—Stony Ridge fault; WTDPFZ—West Tahoe–Dollar Point fault zone. (C) Detail of scarp in Tahoe moraine.

Where fault displacement produces large, dip-slip separations (tens of meters), triangular facets typically separate the offset moraine crests (Fig. 7A). Oblique separation of moraine crests may form trapezoidal facets and offset side slopes (Fig. DR7A [see footnote 1]). Scarps in unconsolidated (cohesionless) moraines may display a "simple" scarp form at one location, whereas nearby along strike, there may be a complex, stepped scarp or a scarp with localized back-tilting (sag) and/or hanging-wall graben, similar to features in faulted alluvium/colluvium along range-front settings (Gilbert, 1890; Slemmons, 1957; Witkind, 1964; Wallace, 1977). Where the deformation is distributed or in younger moraines with smaller displacements, the moraine crest may be draped or warped (e.g., Wallace, 1977).

Extensional Fault-Propagation Folds in Moraines

Most fault segments in the Tahoe-Sierra frontal fault zone have displacement gradients, with displacement approaching zero near fault tips. Near the tips of fault strands and segments, where displacement is small, monoclinal or extensional fault-propagation folds are commonly seen in the unconsolidated glacial cover, above a blind bedrock fault at depth (Figs. 5A and 7E). The displacement gradient along a fault may produce a spectrum of structures, ranging from a gentle monoclinal warp, to a more pronounced step-like fold with footwall antiform and hanging-wall synform (Fig. 7E), to a fully breached monocline where the moraine crest is truncated and the footwall antiform and hanging-wall synform have been offset and are separated by a scarp (Fig. 7A; Fig. DR8A [see footnote 1];

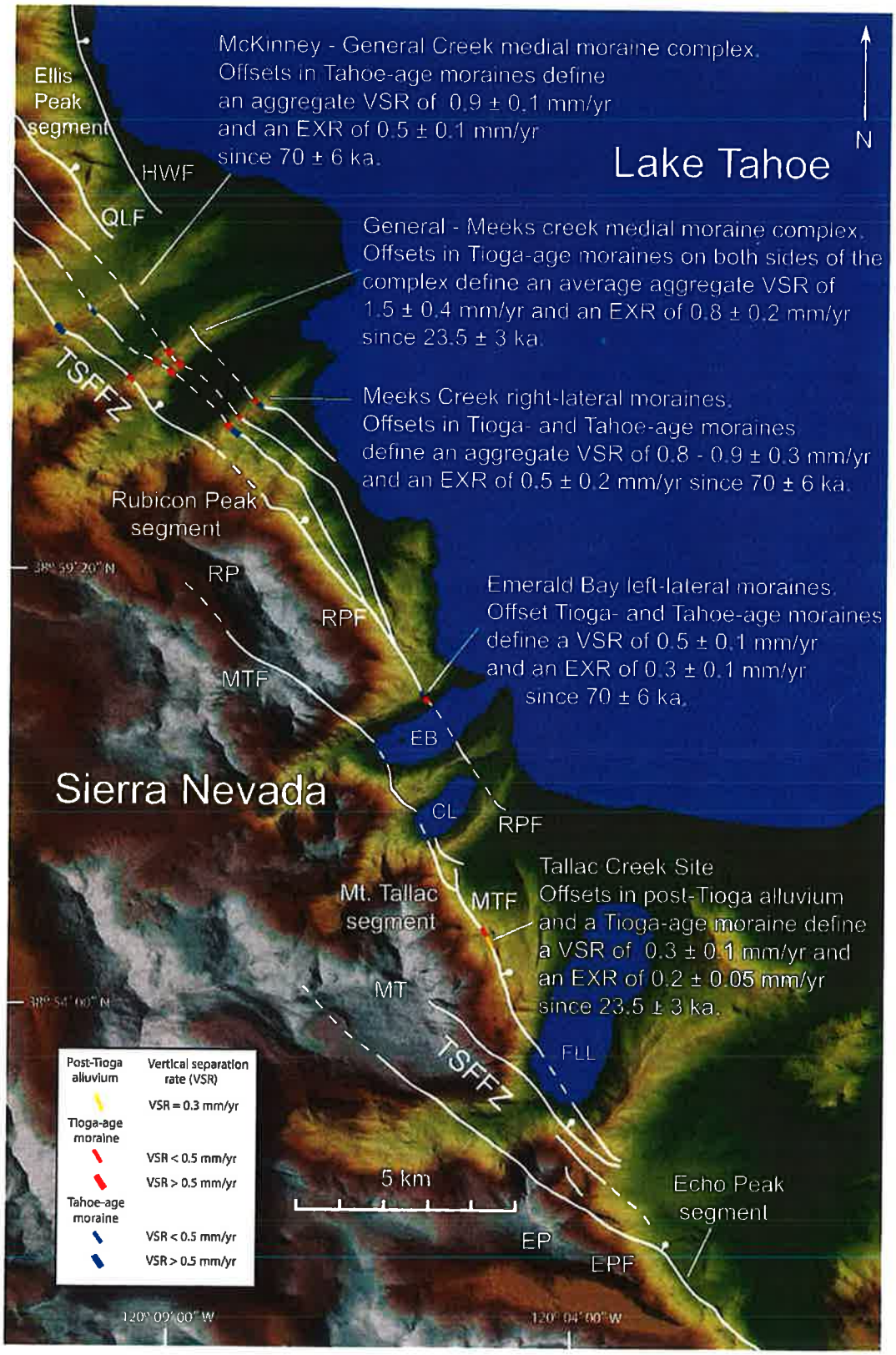

Figure 8.

POTENTIAL EARTHQUAKE MAGNITUDES ALONG THE TAHOE-SIERRA FRONTAL FAULT ZONE

Using published relationships between subsurface-rupture area and observed earthquake magnitudes (Wells and Coppersmith, 1994), we estimated a range of potential earthquake moment magnitudes (M_w) that could be generated by future earthquakes along the Tahoe-Sierra frontal fault zone. Variables incorporated into these rupture scenarios include estimated surface-rupture lengths of 0.7, 0.8, 0.9, and 1.0 times our total mapped fault lengths and depths to the base of the seismogenic zone ranging from 10 km (Hawkins et al., 1986) to 18 km (Smith et al., 2004).

The range-front sections of the Echo Peak and Mt. Tallac faults may have ruptured coseismically in the latest Pleistocene–Holocene time frame, based on 3 m of vertical separation in the Tioga moraine at Osgood Swamp (McCaughey, 2003; Fig. 2), 3.8 ± 0.8 m vertical separation south of Fallen Leaf Lake (Fig. DR12 [see footnote 1]), 3.8 ± 0.9 m vertical separation at the Tallac Creek site (Fig. DR3 [see footnote 1]), and the youthful appearance of the fault scarps at all of these sites. The combined length of the range-front sections of the Echo Peak and Mt. Tallac faults is ~27 km (Fig. 2), which yields a range of potential earthquake magnitudes from 6.5 ± 0.25 to 6.7 ± 0.25. If only the Mt. Tallac fault (with a length of 20 km) were to rupture, earthquake magnitudes could range from 6.3 ± 0.25 to 6.6 ± 0.25 (see Table DR4 [see footnote 1]).

As previously noted, the southern half of the Rubicon Peak segment displaces late Quaternary deposits from southeast of Cascade Lake to the north side of McKinney Creek, a distance of 18 km. North of McKinney Creek, the Rubicon Peak fault projects into the bedrock footwall of the Ellis Peak segment and continues to at least Squaw Valley, another 18 km northwest. Two scenarios for the Rubicon Peak segment are considered herein: rupture of the southern half alone and rupture of the entire mapped length. The first scenario, which considers only that part of the range-front Rubicon Peak fault (fault A; Figs. DR2 and DR5 [see footnote 1]) with evidence of late Quaternary displacement (length of 18 km), yields earthquake magnitudes from 6.3 ± 0.25 to 6.6 ± 0.25 (Table DR5 [see footnote 1]). This part of the Rubicon Peak segment includes the fault splays parallel to the range-front fault (faults B, C, D, and E in Fig. DR5 [see footnote 1]) that we interpret as the complex surface rupture of two or more bedrock faults beneath the unconsolidated piedmont cover. The second scenario, which assumes that the entire mapped length of the Rubicon Peak fault ruptures (length of 36 km; Fig. 2), produces earthquake magnitudes between 6.6 ± 0.25 and 6.9 ± 0.25 (Table DR5 [see footnote 1]).

Comparison of the relatively fresh appearance of post-Tioga side-slope scarps along the Mt. Tallac segment (Fig. 4C) to the degraded and subdued appearance of post-Tioga side-slope scarps along the Rubicon Peak segment (Fig. DR9E [see footnote 1]) suggests that the two segments probably did not rupture coseismically during the last ground-rupturing earthquake along the Mt. Tallac segment. A future coseismic rupture scenario cannot be ruled out, however, because the en echelon right step is <2 km in width (Harris and Day, 1999; Wesnousky, 2006). This scenario has the longest rupture length considered herein but may not be a maximum because we do not include the West Tahoe–Dollar Point fault zone (Fig. 2). The total rupture length of the combined Mt. Tallac and Rubicon Peak faults is 42 km. This surface-rupture length produces a range of earthquake magnitudes from 6.5 ± 0.25 to 6.9 ± 0.25 (Table DR6 [see footnote 1]).

Figure 8 (*on following page*). Summary of vertical separation rates and extension rates along Tahoe-Sierra frontal fault zone. Vertical separation rates (VSR) and extension rates (EXR) discussed in text for major fault strands of the Mt. Tallac and Rubicon Peak segments of the Tahoe-Sierra frontal fault zone (TSFFZ), plotted on U.S. Geological Survey 10 m digital elevation model. Colored fault segments indicate the age of the faulted deposit, and line weights indicate the relative magnitude of the slip rate (see inset legend). Refer to GSA Data Repository Table 3 and Data Repository text for details of individual offsets (see text footnote 1). CL—Cascade Lake; EB—Emerald Bay; EP—Echo Peak; EPF—Echo Peak fault; FLL—Fallen Leaf Lake; HWF—Homewood fault; MT—Mt. Tallac; MTF—Mt. Tallac fault; QLF—Quail Lake fault; RP—Rubicon Peak; RPF—Rubicon Peak fault.

POSSIBLE EARTHQUAKE-TRIGGERED LANDSLIDES ALONG THE TAHOE-SIERRA FRONTAL FAULT ZONE RANGE FRONT

Rotational landslides and translational rockslides in close proximity to the mapped Mt. Tallac fault occur along the Mt. Tallac range front at the heads of Fallen Leaf Lake, Cascade Lake, and Emerald Bay (Fig. DR1 [see footnote 1]). Similarly, from Emerald Bay northwest along the oversteepened slope at the base of the Rubicon Peak range front, numerous landslides straddle and/or lie adjacent to the mapped range-front fault (Figs. DR2 and DR5 [see footnote 1]). In several places, fault scarps coincide with landslide head scarps, and in other places, the landslide deposits have been displaced by the Rubicon Peak fault. The close proximity of these mass-wasting features with mapped faults strongly suggests that they have been triggered by strong ground motion during earthquakes along the Tahoe-Sierra frontal fault zone.

CONCLUSIONS

The bare-earth LiDAR topography reveals a broad array of tectonic geomorphic features along the Tahoe-Sierra frontal fault zone west of Lake Tahoe, demonstrating late Pleistocene to Holocene activity along the fault zone and validating earlier mapping of the fault zone (Schweickert et al., 2000, 2004). This study utilized bare-earth LiDAR data, together with field data to identify, visualize, and characterize faults in a mountainous and heavily forested region. The tectonic geomorphic features of faulted lateral moraines described herein and illustrated with the bare-earth LiDAR imagery provide clearly defined examples for studies of range-front lateral moraines displaced and disrupted by normal faults elsewhere. The examples highlight the unique geomorphic features that develop in relatively thick unconsolidated lateral moraines above an imbricate bedrock fault zone away from the range front. This study also presents new three-dimensional methods utilizing the bare-earth LiDAR point cloud data for modeling tectonic displacements of range-front alluvium, colluvium, and glacial moraine crests. These methods have yielded statistically robust estimates of vertical separation and extension across fault arrays at 17 locations.

New terrestrial cosmogenic nuclide and optically stimulated luminescence age data from the study area have been combined with regional age data to establish limiting ages for the Tioga (23.5 ± 3 ka) and Tahoe (70 ± 6 ka) glaciations in the Lake Tahoe region, which correlate with marine isotope stages MIS 2 and MIS 4, respectively.

We coupled these numerically robust displacement models with the new age estimates to define vertical separation and extension rates at numerous localities for the past ~70 k.y. This data set on vertical separations and extensions

Stop 3-4: Grover Hot Springs. Camp for the night and enjoy the hot springs!

Day 4: Leave Grover and drive south and east to Hwy 395. Drive south through the Owens Valley and back to Northridge.

Day 4-1 (time permitting): View moraines at Convict Lake.

ROBERT P. SHARP *Division of Geological and Planetary Sciences, California Institute of Technology, Pasadena, California 91109*

Pleistocene Glaciation, Bridgeport Basin, California

ABSTRACT

Bridgeport Basin, east of the Sierra Nevada in central California, contains deposits of the following Pleistocene glaciations, youngest to oldest: Tioga, Tenaya, Tahoe, Mono Basin, and Sherwin(?). Some evidence also suggests an advance between the Mono Basin and Sherwin(?). With respect to the last major interglacial, the first three glaciations are younger, position of the Mono Basin is debatable, and the others are older.

The following conclusions have been drawn. (1) Within Bridgeport Basin, Sherwin(?) glaciers were the most extensive. (2) Since Sherwin(?) time, warping and erosion have caused significant topographic changes in the piedmont area at the east Sierra foot. (3) Bridgeport Valley has been warped down relative to the range front and northward tilting of the piedmont has reversed a stream formerly flowing south into Mono Basin. (4) A gravel filling of Bridgeport Valley occurred to a depth of at least 250 ft (75 m), and locally twice that amount, at about the same time as the Sherwin(?) glaciation. Most of this fill is believed to have been warped down and covered by modern alluvium. (5) Gravels, at least 500 ft (150 m) thick, were also deposited in nearby Huntoon Valley in Sherwin(?) time, at least in part, because of meltwater overflow from a large pool of glacier ice occupying West Walker River. (6) Eastward flow of ice out of Robinson Creek during Mono Basin time built a moraine that escaped burial by the subsequent more extensive Tahoe glacier that flowed north along the present course of Robinson Creek. This fortuitous circumstance facilitates recognition of the Mono Basin glaciation. (7) Ice from Robinson Creek also flowed eastward through the Summers Meadows trough in Sherwin(?) time and probably also within the interval between the Sherwin(?) and Mono Basin glaciations. (8) The Tahoe glaciers of Robinson and Buckeye Creeks coalesced to form a piedmont bulb. (9) Qualitative relations and semiquantitative data indicate that the Tenaya is a valid and distinct glaciation between Tahoe and Tioga, although the small moraines suggest that it was a relatively short-lived event. (10) The size and spacing of recessional moraines demonstrate a reasonably consistent but not identical behavior of Tioga ice streams in the four principal canyons of Bridgeport Basin.

INTRODUCTION

Introductory Statement

Pleistocene glacial deposits in Bridgeport Basin, mostly moraines, were described by Blackwelder (1931) in his classical reconnaissance of Sierra Nevada glaciations. Results of a more detailed investigation and mapping of deposits of the Tioga, Tenaya, Tahoe, Mono Basin, and Sherwin(?) glaciations, and of a possible intermediate ice advance in Bridgeport Basin, are reported here. This study provides semiquantitative data that indicate the Tenaya is truly a separate glaciation between Tioga and Tahoe. It treats evidence for the pre-Tahoe and post-Sherwin glaciation, earlier named Mono Basin (Sharp and Birman, 1963), and describes relations indicating an intermediate glaciation within the Mono Basin–Sherwin(?) interval. Particular attention is given to relations suggesting significant post-Sherwin(?) changes in landscape through deformation, erosion, and deposition. The query after Sherwin indicates lack of definite correlation with the type locality at Rock Creek (Fig. 1). Blackwelder (1931) assigned these Bridgeport Basin deposits and features to Sherwin, and that appears a suitable working designation for the present, but with a query to indicate uncertainty.

An extended discussion of the sequence of Pleistocene glaciations in the central Sierra Nevada is not an objective here, but the accompanying tabulation and comments are provided for readers unfamiliar with the region. Table 1 is adapted with modifications

Geological Society of America Bulletin, v. 83, p. 2233–2260, 22 figs., August 1972

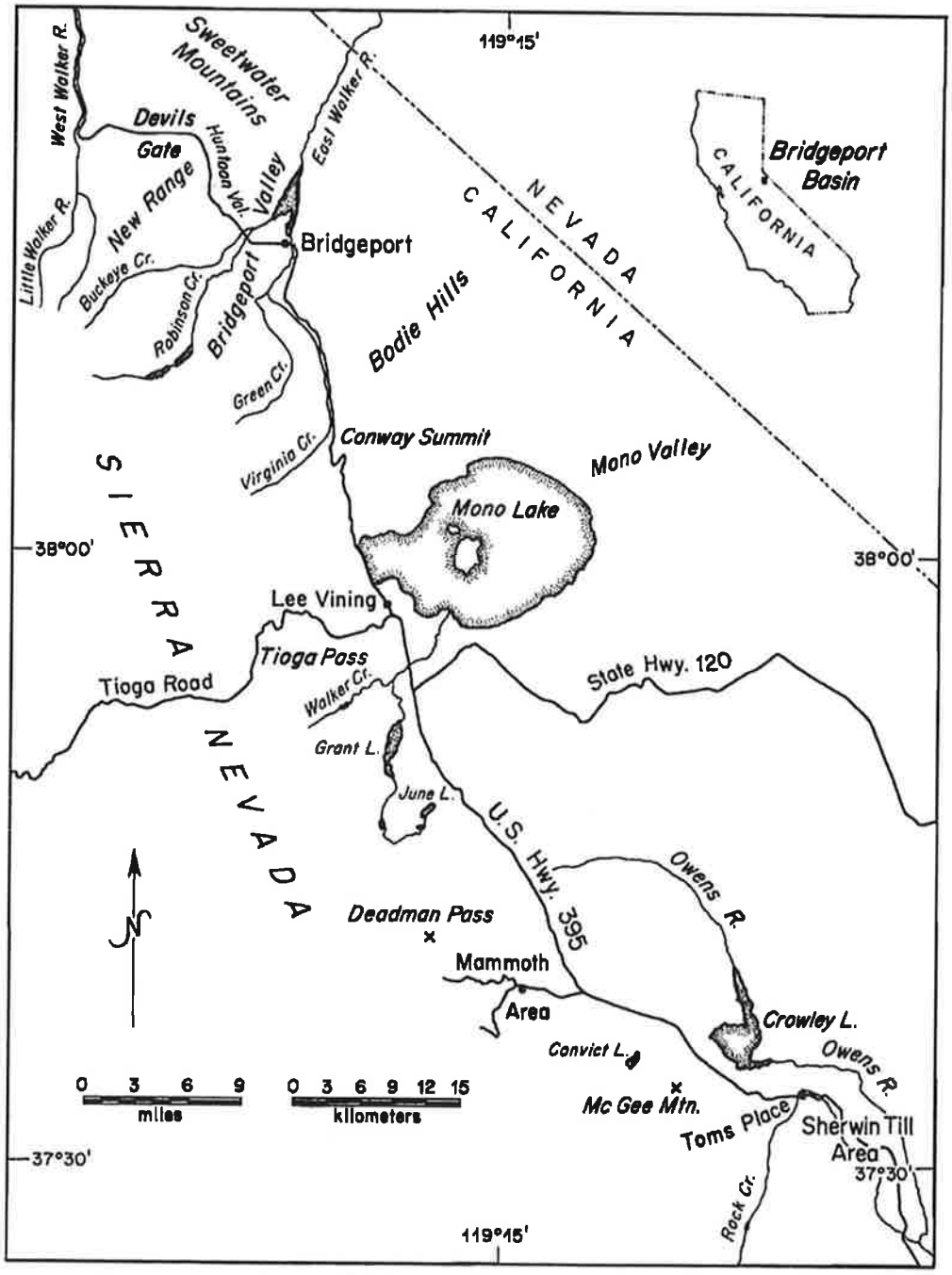

Figure 1. Regional geographical features and localities, east-side central Sierra Nevada.

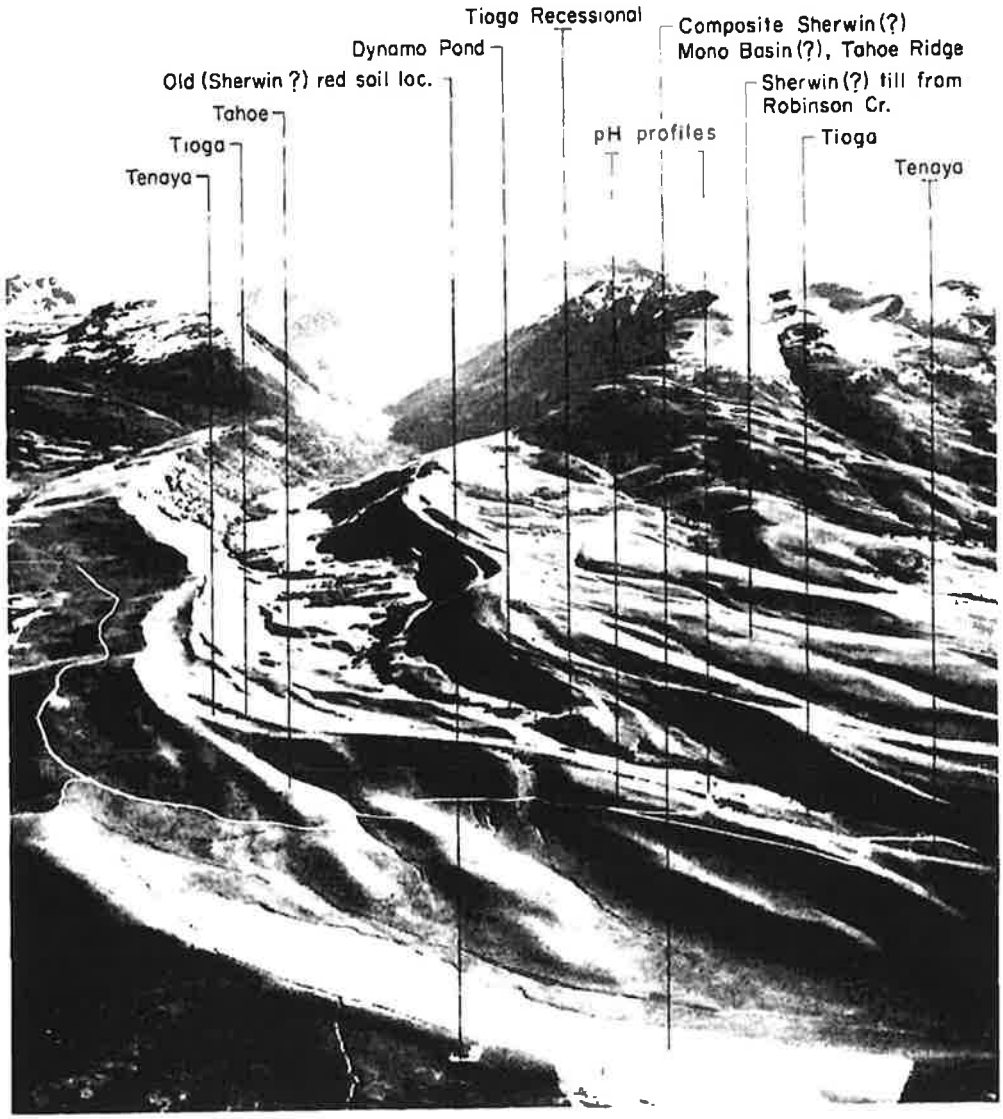

Figure 6. Oblique air photo of moraines on lower Green Creek taken by John S. Shelton (4869).

sides of lowermost Green Creek, the Tahoe laterals rest upon older Sherwin(?) and intermediate tills.

Birkeland and Janda (1971) show that clay minerals in soils on most glacial deposits along the east base of the central Sierra Nevada are not particularly sensitive indicators of age. Here on Green Creek, color and *p*H profiles within the weathered layer are modestly different for Tioga and Tahoe deposits (Fig. 8). Neutral conditions (*p*H 7) attain at a shallower depth in the Tioga, 48 compared to 168 inches (122 and 427 cm), and brownish colors extend much deeper in the Tahoe, 300 compared to 48 in. (762 and 122 cm).

Robinson Creek

Description. The more significant glacial deposits of Robinson Creek lie between Lower Twin Lake and the canyon mouth (Fig. 9). This 4-mi (6 km) stretch of open, U-shaped valley bears nearly due north, and its west

WALKER LANE FIELD TRIP GUIDE

Compiled by Cathy Busby, Department of Earth Science, University of California Santa Barbara CA

for

BASINS GRADUATE CLASS FIELD TRIP
Jackson School of Geosciences, University of Texas at Austin
Ron Steel and Brian Horton
April 21 – 25, 2011

GUEST FIELD TRIP LEADERS:
Pat Cashman and Jim Trexlor, University of Nevada Reno (Day 1)
Graham Kent, University of Nevada Reno (Day 1)
Angela Jayko, U.S. Geological Survey (Day 2)
Dave Wagner, California Geological Survey (Day 3)
Ian Norton, UTIG, Jackson School (Day 4)

OTHER JACKSON SCHOOL PARTICIPANTS:
Liz Catlos, Pat Dickerson, Ethan Lake

Color figures are at the back of the guidebook; black and white figures are interspersed.

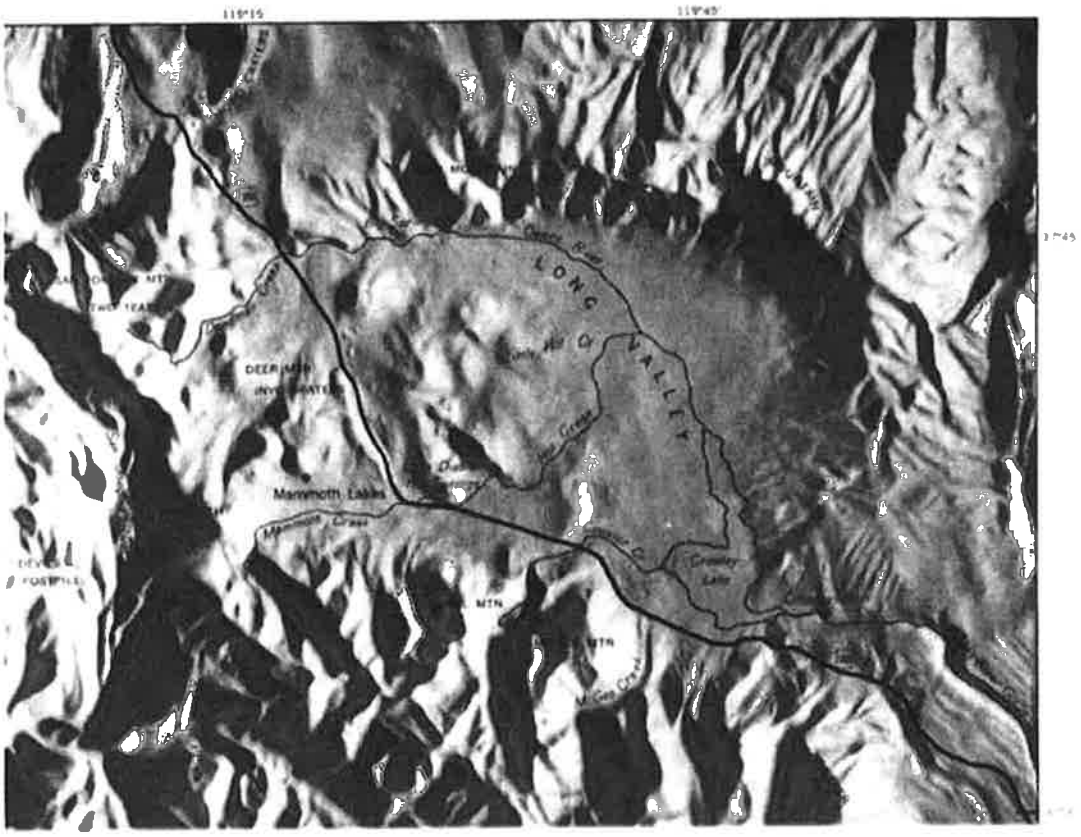

Fig. 2. Shaded relief map of Long Valley caldera.

DAY TWO FIGURE 9 (above): Long Valley shaded relief map.

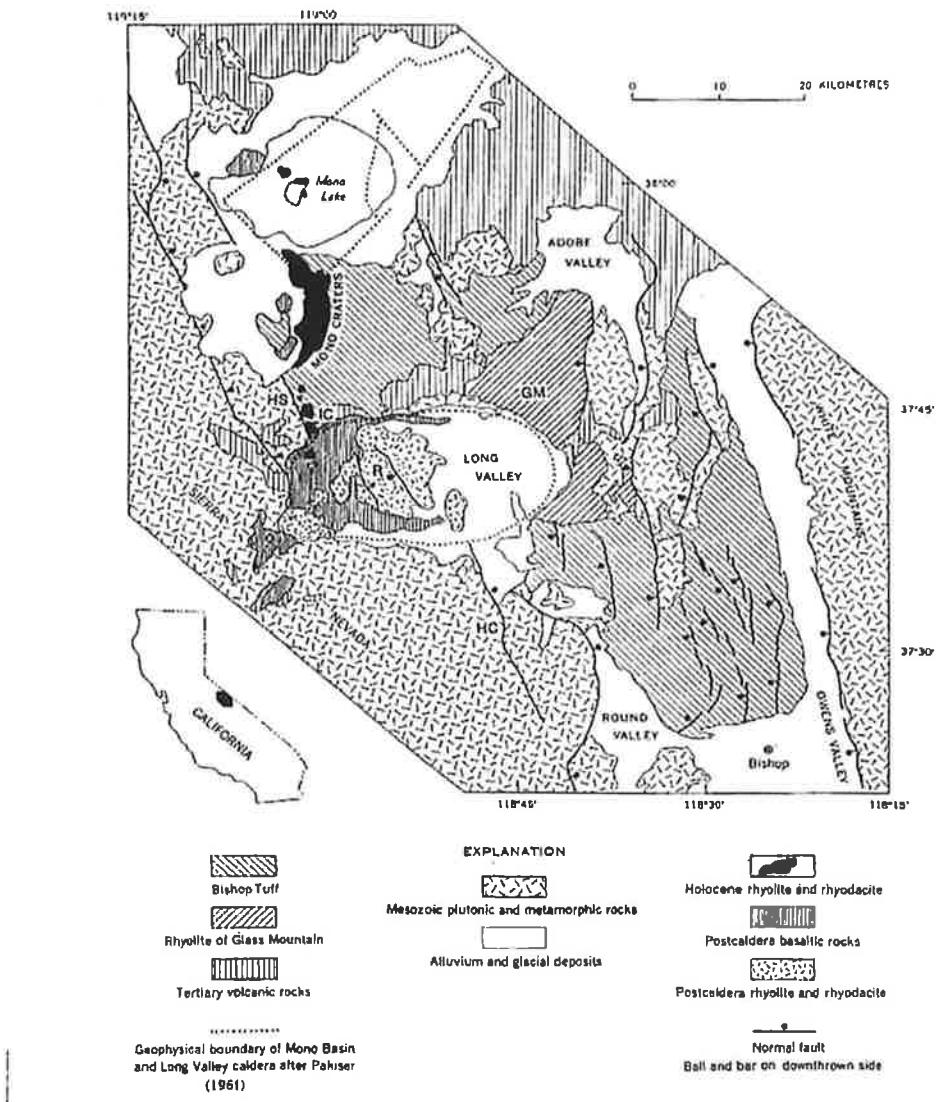

Figure 18. *Generalized geologic map of Long Valley-Mono Basin region. The Volcanic Tableland is the area of Bishop Tuff between the Long Valley caldera and the town of Bishop. GM = Glass Mountain Ridge; HC = Hilton Creek fault; HS = Hartley Springs fault; IC = Inyo Craters; R = resurgent dome of Long Valley caldera and its medial graben. (Modified from Bailey and others, 1976, Jour. Geophys. Research, © American Geophysical Union)*

DAY TWO FIGURE 10 (above): Generalized geologic map of the Long Valley – Mono Basin region.

OPTIONAL STOP (1:00 – 3:00 pm)–Inyo Craters (about 2 hours)

Turn right (west) on Dry Creek Road "Mammoth Scenic Loop" which was built to provide an escape route for Mammoth Lakes in case of a volcanic eruptions. Go 3 miles, and turn right onto a dirt road leading to a parking area for Inyo Craters. From the parking lot, walk a quarter mile walk to the craters. There are three craters here, all aligned a northerly axis, but here we can see the two southern craters, termed "North" and "South." These pits are about 600 ft in width and 180 ft deep. The craters are the result of violent steam explosions. where rising molten magma contacted groundwater. The three explosions occurred at roughly the same time, possibly within hours or days (Bailey, 1989). An age of 710 years for the craters is based on age-dating of a shattered log in South Crater.

Return to Mammoth Scenic Route, continue south to highway 203 and turn left, through Mammoth Lakes, and return to Highway 395 south.

Casa Diablo Hot Springs and Geothermal Area
This is at **the intersection of highway 203 and highway 395**. It is located on the southern edge of the resurgent dome along a NW-trending fault within the medial graben. It was the site of seismic swarms of 1980-1983. There are three power plants at this site: one 10-megawatt and two 15-megawatt plants, using hot water from a reservoir about 600 feet deep.

To the west is Mammoth Mountain volcano, which lies on the western rim of the caldera and is about 400,000 years old.

Lake Crowley is formed by a dam that blocks the outlet to the Owens River. The trace of the south edge of the Long valley caldera runs through the north end of the lake.

LOOK UP TO THE RIGHT (WEST) to see the **Hilton Creek fault** (HC, Figure 2 – 10) forming a 50' high planar scarp on Tahoe age lateral moraine along McGee Creek (see Figure 2 – 11). Clark (1981 found the latest Tioga tills (10,000 - 25,000 years, Late Wisconsin) to be offset over 50' and Tahoe tills (60,000-130,000 years, Early Wisconsin) have been offset about 400'. Clark and others (1980) mapped surface disturbances along the fault which they contribute to fault displacement during the May, 1980 seismic events, but they were very small. Furthermore, surface expression of the fault is lost to the north where it goes into the Long Valley caldera (Figure 2 – 10). This is probably because it gets injected by magma there, and it is thought that magma injection may have caused some of the 1980 earthquakes.

Fault scarp offsetting Tahoe age glacial moraines along McGee Creek. The scarp is about 60 feet high and aligns perfectly with the Sierran range front.

DAY TWO, FIGURE 11

Continue south to Sherwin Summit (elevation 7,000'). 0.5 miles beyond the summit is the big roadcut in Sherwin Till. Drive another 0.3 miles and park along right shoulder of highway.

DAY TWO continued - STOP: THE BIG PUMICE CUT

This is one of the most famous road cuts in California, because when it was in cut in 1957, it provided an exposure of glacial till overlain by 760,000 old Bishop Tuff. However, in his 1938 PhD thesis, one of my professors at Berkeley, Charles Gilbert, first recognized glacial till beneath the Bishop Tuff in the Owens River Gorge, and concluded that it was Sherwin Till. (In that PhD thesis, he also recognized that the Bishop Tuff is an ignimbrite – in an era where only a handful of geologists understood the origin of ignimbrites). The roadcut's condition has deteriorated, even since I started looking at it in the 1970's, so this may be a very quick stop.

The till is estimated to have undergone about 50,000 to 70,000 years of weathering prior to burial, so it is probably about 800,000 years old (Sharp and Glazner, 1997). This makes it correlative with the Kansan glacial stage of the mid-continent U.S. The bouldery, bush-dotted lower part of the cut is the till; boulders in it largely decomposed to grus (rotted granite). It is overlain by 75 feet of white pumiceous rock. The basal 15' is relatively fine-grained and bedded, and mantles the till, so it is probably a fall deposit. The upper 60' is unsorted, with larger pumices, and is more massive (with very faint horizontal stratification), so it is a pyroclastic flow deposit. The till and the white pumiceous rock are cut by clastic dikes, which coarsen upward toward (and end at) Pleistocene fluvial gravels at the top (from which they were likely derived).

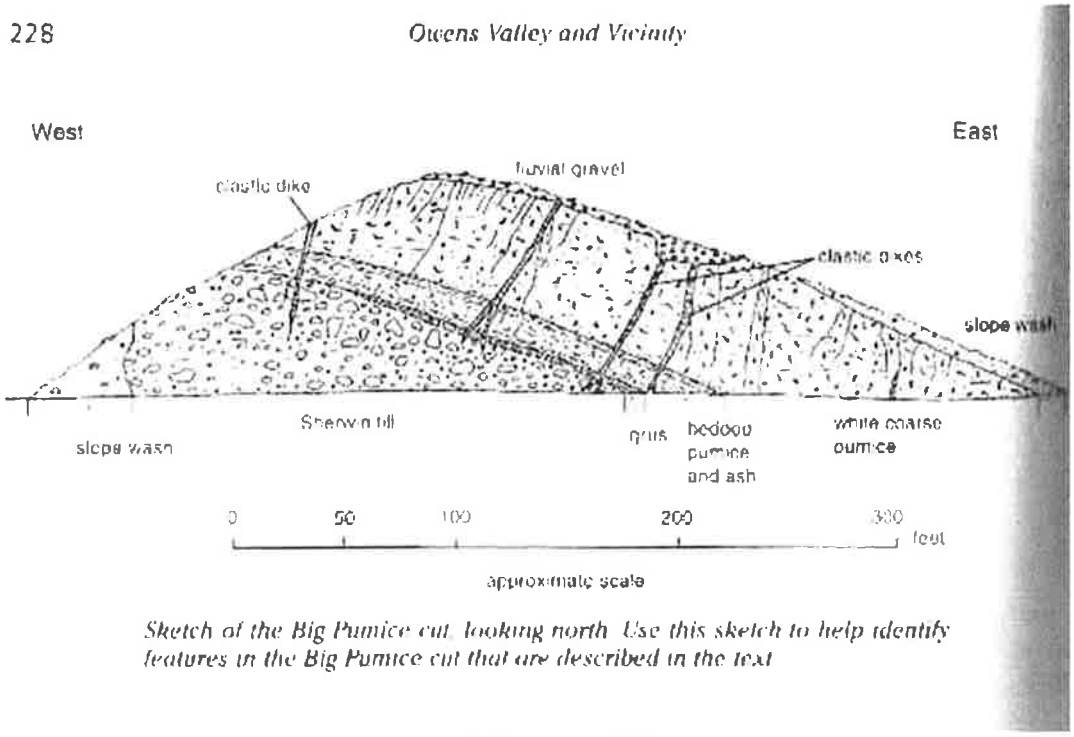

Sketch of the Big Pumice cut, looking north. Use this sketch to help identify features in the Big Pumice cut that are described in the text

DAY TWO, FIGURE 12 from Sharp and Glazner, 1997.

Day 4: Convict Lake Moraines
Highway 395, Owens Valley

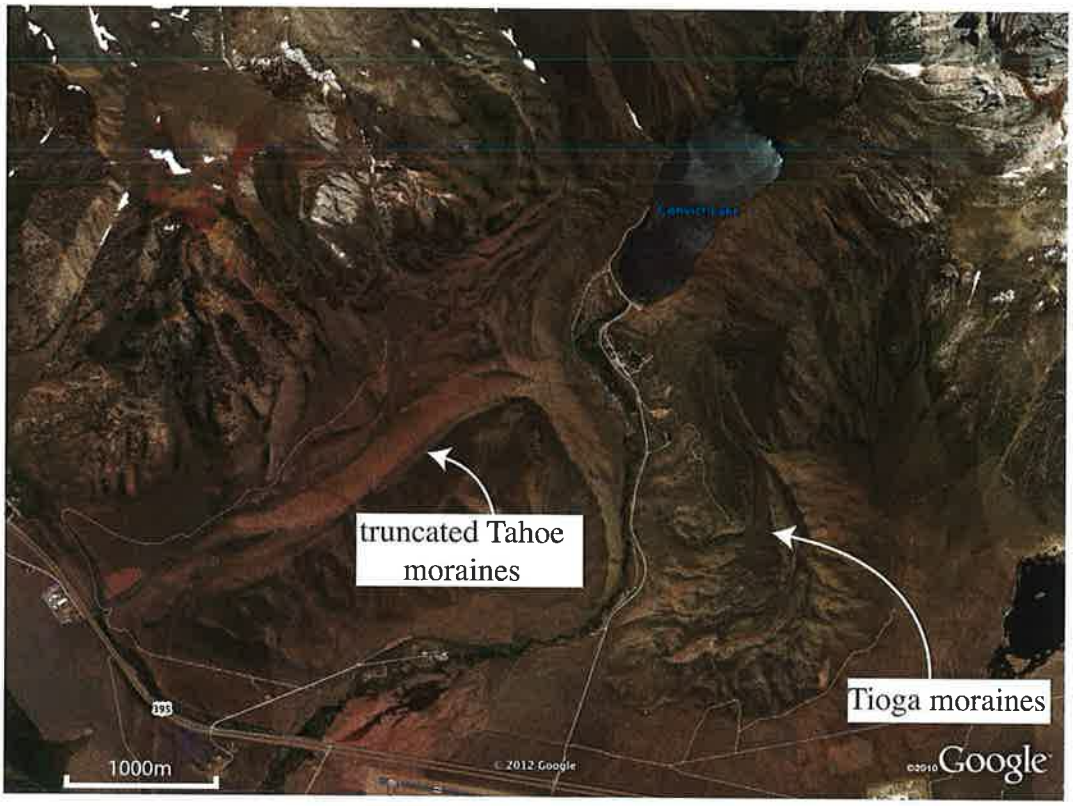

Google Earth image of Convict Lake.

Oblique aereal photograph looking west up towards Convict Lake.